SKELETAL DEFICITS IN MALE AND FEMALE MOUSE MODELS OF DOWN SYNDROME

by

Jared Thomas

A Thesis

Submitted to the Faculty of Purdue University

In Partial Fulfillment of the Requirements for the degree of

Master of Science

Department of Biology at IUPUI

Indianapolis, Indiana

May 2020

THE PURDUE UNIVERSITY GRADUATE SCHOOL
STATEMENT OF COMMITTEE APPROVAL

Dr. Randall J Roper, Chair

School of Science, Department of Biology

Dr. Jiliang Li

School of Science, Department of Biology

Dr. Joseph M Wallace

School of Engineering and Technology, Department of Biomedical Engineering

Dr. James Marrs

School of Science, Department of Biology

Approved by:

Dr. Theodore Cummins, Ph.D.

For my husband, Loïc who has been my champion and my family who has always believed in me

ACKNOWLEDGMENTS

Thank you to Dr. Randall J Roper for all his support, guidance, and patience. His mentorship has given me the opportunity to become a researcher, confidence to further pursue my education, and created a great lab family. Thank you to Dr. James Marrs and Dr. Jiliang Li for serving on my graduate committee and helping me become a better researcher and student. Also, thank you to Dr. Joseph Wallace for serving on my committee, his assistance with biomechanical testing, and microCT analysis. A special thank you to Dr. Keith Condon and Drew Brown of the Histology Core of the IU School of Medicine for their expertise and training in histologic techniques. To my current and past labmates, Irushi Abeysekera, Gracelyn Bose, Emily Hayley, Jonathan LaCombe, Laura Hawley, Adam Knox, Anna Brehend, Kourtney Sloan, and Matthew Blackwell for all their help and support. Your encouragement and friendship has been invaluable to me and it has been a pleasure working with you all.

TABLE OF CONTENTS

LIST OF TABLES

LIST OF FIGURES

ABSTRACT

Down syndrome (DS) is a genetic disorder that results from triplication of human chromosome 21 (Hsa21) and occurs in around 1 in 1000 live births. All individuals with DS present with skeletal abnormalities typified by craniofacial features, short stature and low bone mineral density (BMD). Differences between males and females with DS suggest a sexual dimorphism in how trisomy affects skeletal deficits associated with trisomy 21 (Ts21). Previous investigations of skeletal abnormalities in DS have varied methodology, sample sizes and ages making the underlying causes of deficits uncertain. Mouse models of DS were used to characterize skeletal abnormalities, but the genetic and developmental origin remain unidentified. Over-expression *Dyrk1a*, found on Hsa21 and mouse chromosome 16 (Mmu16) has been linked to cognitive deficits and skeletal deficiencies. Dp1Tyb mice contain three copies of all of the genes on Mmu16 that are homologous to Hsa21, males and females are fertile, and therefore are an excellent model to test the hypothesis that gene dosage influences the sexual dimorphism of bone abnormalities in DS. Dp1Tyb at 6 weeks 16 weeks showed distinctive abnormalities in BMD, trabecular architecture, and reduced bone strength over time that occur generally through an interaction between sex and genotype. Increased gene dosage and sexual dimorphism in Dp1Tyb mice revealed distinct phenotypes in bone formation and resorption. To assess how *Dyrk1a* influences the activity and function of osteoblasts Ts65Dn female trisomic mice, female mice with a floxed *Dyrk1a* gene (Ts65Dn, $Dyrk1a^{fl/+}$) were be bred to *Osx1*-GFP::Cre+ mice to generate Ts65Dn animals with a reduced copy of *Dyrk1a* in mature osteoblast cells. Female Ts65Dn,$Dyrk1a^{+/+/+}$ and Ts65Dn,$Dyrk1a^{+/+/-}$ displayed significant defects in both trabecular architecture and cortical geometry. Ultimate force was reduced in trisomic animals, suggesting whole bone and tissue level properties are not adversely affected by trisomy. Reduction of *Dyrk1a* functional copy number in female mice did not improve skeletal deficits in an otherwise trisomic animal. *Dyrk1a* may not alter osteoblast cellular activity in an autonomous manner in trisomic female mice. These data establish sex, gene dosage, skeletal site and age as important factors in skeletal development of the skeleton in DS mice, potentially paving the way for identification of the causal dosage-sensitive genes in both male and female animals.

CHAPTER 1. INTRODUCTION

1.1 Down Syndrome

Down syndrome (DS) is the most common genetic cause of intellectual disability and the result of the triplication of human chromosome 21 (Hsa21) (Turpin & Lejeune, 1965). Most cases of Trisomy 21 (Ts21) results from non-disjunction of Hsa21 during meiosis as a freely segregating chromosome or a Robertsonian translocation (Epstein, 2014). Additionally, DS can result from partial trisomies where a portion of Hsa21 genes are triplicated or mosaicism with trisomy of Hsa21 in some cells and two copies of Hsa21 in other cells. Phenotypes associated with partial trisomies or mosaics vary in severity depending on the number and distribution of trisomic genes and cells respectively. The only identified risk of DS is associated with the age of the mother by analyzing the rates of non-disjunction during gamete formation (Hernandez & Fisher, 1996). Ts21 affects ~1/800 to 1/1000 live births and results in distinctive craniofacial features and skeletal deficits, including short stature in all individuals with DS (Baptista, Varela, & Sardinha, 2005; Center, Beange, & McElduff, 1998; Gonzalez-Aguero, Vicente-Rodriguez, Moreno, & Casajus, 2011; Mai et al., 2019; McKelvey et al., 2013; Parker et al., 2010). Phenotypic variability and severity in individuals with DS are poorly understood and it is necessary to investigate the molecular and genetic factors that contribute to the skeletal phenotype in individuals with DS.

Alterations in skeletal features in individuals with DS begin prenatally and continue postnatally; adolescents exhibit low bone accrual during puberty, and adults have documented bone loss (Angelopoulou, Souftas, Sakadamis, & Mandroukas, 1999; Baptista et al., 2005; Gonzalez-Aguero et al., 2011). Fetuses with Ts21 are often characterized ultrasonically with a short femur and humerus, but these soft markers are not diagnostic (Bromley, Lieberman, Shipp, & Benacerraf, 2002a, 2002b; Longo, DeFigueiredo, Cicero, Sacchini, & Nicolaides, 2004; Nyberg et al., 2001). At birth, individuals with DS have a shorter stature than the general population (Cronk et al., 1988; Myrelid, Gustafsson, Ollars, & Anneren, 2002) and on average, this reduced height continues throughout life (Baptista et al., 2005). The short stature caused by Ts21 is related to a delay in the development of the secondary centers of ossification and final peak height reached around the age of 15 (Angelopoulou et al., 1999; de Moraes, Tanaka, de Moraes, Filho, & de Melo Castilho, 2008). Peak bone mass is reached ~5-10 years earlier than normal and is lower in

individuals with DS as compared to the general population (Costa et al., 2018). This predisposition to weaker and shorter bones in people with Ts21, through attenuated bone accrual or altered organization, may be exacerbated due to hypotonia, hormonal and nutritional deficits, growth retardation, low muscle strength and reduced physical activity (Carfi et al., 2017; Esbensen, 2010; Hawli, Nasrallah, & El-Hajj Fuleihan, 2009).

1.1.1 History of Down syndrome

Around the mid-19th century, DS was first mentioned in Jean-Etienne-Dominique-Esquirol's first handbook of psychiatry entitled "Des maladies mentales considerées sous les rapports medical, hygienique et medico-legal (Mental Disease: medical, health/hygiene and medical-legal considerations" (Esquirol & Hunt, 1845; Patterson & Costa, 2005). "Idiocy" was a section in his handbook that characterized 'mental deficiency or retardation', accompanied by physical characteristics including patients with oblique eye fissures, epicanthic eye-folds, a flat nasal bridge, short stocky nature, malformed limbs and protruding tongue (Esquirol & Hunt, 1845; Roubertoux & Kerdelhue, 2006). Edouard Seguin added to the symptomatological description of these patients, around 8 years later, by adding small nose, open mouth and the morphology of the tongue and susceptibility of lung infections (Roubertoux & Kerdelhue, 2006; Seguin, 1866). He believed that these "good kids" had the ability to communicate and gain some basic knowledge despite "profound idiocy" (Seguin, 1866). It also has been suggested that advancement in understanding of the cause of DS parallels the history of human genetics (Patterson & Costa, 2005). In 1866, at the mental hospital where John Langdon Down was working, he separated his patients into ethnic groups, and stated "A very large number of congenital idiots are typical Mongols" (Roubertoux & Kerdelhue, 2006). This description referred to Langdon's perspective that patients with DS appeared to have similar facial features as individuals from Mongolia. He added to the phenotype of DS by noting a flat broad face, scanty hair, small nose, and long, thick protruding roughened tongue (Down, 1995). He stated they had the ability to speak, although their speech was inarticulate, also they had a great sense of humor. With training individuals with DS could improve their speech, motor functioning, physical and mental capabilities, and possessing a reduced life expectancy (Roubertoux & Kerdelhue, 2006).

The term "Mongol" or "mongolism" was used to describe features of individuals with DS and was used commonly by the 19th century and until the 1960s. (Patterson & Costa, 2005;

Roubertoux & Kerdelhue, 2006). It was viewed as a derogatory term used to describe DS and thought to be a non-scientific etiology. Individuals petitioned the World Health Organization (WHO) to formally request the term *'Mongol'* and *'mongolism'* be eschewed and was established by the National Institute of Health (NIH) in 1975 (Howard-Jones, 1979; Patterson & Costa, 2005; Roubertoux & Kerdelhue, 2006). Individuals in the scientific community suggested the term be discarded and replaced with either *"trisomy 21 anomaly"* or *"Down's syndrome"* which became common parlance in the 1970s (Howard-Jones, 1979; Patterson & Costa, 2005; Roubertoux & Kerdelhue, 2006).

During the early to mid-20th century, several scientists discovered chromosomes and their behavior during cell division. Thomas H. Morgan published several studies that provided almost conclusive evidence that genes are located on chromosomes (Patterson & Costa, 2005). Early investigations into number of chromosomes yielded evidence that humans had around 46 chromosomes (Patterson & Costa, 2005) and that lead Charles Davenport to consider that the cause of intellectual disabilities was a chromosomal irregularity. Following the discovery of the correct number of human chromosomes Jerome Lejeune showed that DS was the result of triplication of Hsa21 (Patterson & Costa, 2005).

1.1.2 Genotype and Phenotype Relationship

DS is the most compatible genetic chromosomal anomaly with human survival past term (Olson et al., 2007). DS phenotypes are highly variable and have considerable genetic complexity, thus making it difficult to understand mechanisms related to developmental disruption by Ts21 (Olson et al., 2007). Majority of the incidence of DS results from Ts21 and some from translocations of portions of Hsa21 on other chromosomes (S .L. Deitz, Blazek, Solzak, & Roper, 2011; Epstein, 2014). Also, some individuals with DS phenotypes have Ts21 in only a portion of their cells (mosaicism) while other cells have the normal number of chromosomes (S .L. Deitz et al., 2011; Epstein, 2014). Cellular and genetic composition in individuals with DS contribute to differences in variation and severity of observed phenotypes. It has been hypothesized that specific trisomic genes or chromosomal regions may cause or alter DS phenotypes due to genotype-phenotype correlations (S .L. Deitz et al., 2011). It is still unclear how genetic mechanisms of Ts21 result in various phenotypes seen in DS, yet it is unlikely that a single mechanism is responsible for the etiology of all Ts21 phenotypes. Identification of the genetic mechanisms affecting DS

phenotypes that are influenced by differential spatiotemporal gene expression in various tissues can lead to therapeutics that could correct distinct DS phenotypes (Conti et al., 2007; Lintas et al., 2010; Lyle et al., 2004; Moldrich et al., 2007).

The most common techniques used in the investigation into a relationship between genotype-phenotype correlations included mapping of partial trisomies, mouse models, studying gene expression in tissues or cells, and transgenic mice overexpressing one gene. From these investigations, the distal arm of Hsa21 was thought to be sufficient to cause phenotypes associated with DS (Patterson & Costa, 2005). It was hypothesized that specific regions on Hsa21 resulted in specific phenotypes and that the extent of the trisomic region relates to the variation and severity of traits associated with DS (Delabar et al., 1993; Korenberg et al., 1994; McCormick et al., 1989; Niebuhr, 1974).

Gene Dosage Hypothesis

The central hypothesis in DS research is that gene expression is elevated by 50% or 1.5 fold as a result from increased gene dosage which alters development of individuals with DS (Amano et al., 2004; K. Gardiner, 2004; Kahlem et al., 2004). Based on the assumption that a gene present in three copies results in elevated expression, two principal hypotheses of how Ts21 causes DS were proposed. The first hypothesis of the genotype-phenotype relationship was that genomic imbalance caused DS phenotypes (Patterson & Costa, 2005). The genetic dosage imbalance hypothesis suggests that increased copy number or dosage on Hsa21 genes would lead to increased gene expression or protein (Antonarakis, Lyle, Dermitzakis, Reymond, & Deutsch, 2004; Epstein, 2014). Overexpression of dosage sensitive genes would lead to DS phenotypes and specific genes or subsets of genes are sufficient cause specific phenotypes (S .L. Deitz et al., 2011; Patterson, 2007). Further investigations have highlighted that changes in gene expression may be specific to a particular tissue at a precise developmental or mature stage (S .L. Deitz et al., 2011).

Amplified Genetic Instability

The second hypothesis is amplified developmental instability that refers to the phenomenon observed when an increased dosage of a number of trisomic genes leads to genetic imbalance that impacts the expression and regulation of many genes throughout the genome (S .L. Deitz et al.,

2011; Pritchard & Kola, 1999). The presence of an extra chromosome is assumed to result in the disruption of genetic homeostasis throughout the genome, possibly affecting various signaling pathways associated with phenotypes observed in DS (S .L. Deitz et al., 2011; Patterson, 2009). This hypothesis is an attempt to explain the observations of DS traits that are similarly seen in other aneuploid states and normosomic people. Therefore, it has been hypothesized that changes in global genomic expression caused by Ts21 can lead to DS phenotypes (S .L. Deitz et al., 2011). The severity and incidence of phenotypes associated with DS is thought to be dependent on the number of trisomic genes, and that phenotypes are associated to changes in genetic expression in the entire chromosomal domain (K. J. Gardiner, 2010).

Down Syndrome Critical Region

Studies of individuals with chromosomal rearrangements that resulted in triplication of a subset of Hsa21 genes or segmental trisomy were used to identify similarities in phenotypes with individuals with DS (Olson et al., 2007; Patterson & Costa, 2005; Roubertoux & Kerdelhue, 2006). Correspondence of a region of overlap between patients with DS that possessed the same phenotypes led to a concept that a critical chromosomal region of dosage sensitive genes was responsible for various phenotypes associated with DS (Delabar et al., 1993; Korbel et al., 2009; Olson et al., 2007). The Down syndrome critical region (DSCR) contained approximately 33 genes found on Hsa21 (Olson, Richtsmeier, Leszl, & Reeves, 2004). The DSCR included *Dyrk1a* and was thought to contribute to the most severe features of DS (Korbel et al., 2009; Korenberg et al., 1994; Richtsmeier, Zumwalt, Carlson, Epstein, & Reeves, 2002). The hypothesis suggested that the genes in this region were sufficient to engender these phenotypes. Further investigations concluded that genes located within the DSCR were insufficient but necessary to produce phenotypes associated with DS (S. L. Deitz & Roper, 2011; Olson et al., 2007). However, specific regions or genes may contribute to the incidence and severity of specific DS phenotypes (Korbel et al., 2009; Lyle et al., 2009), leading to the idea that increased gene dosage could generate susceptibility regions that influence particular phenotypes through interactions between trisomic and non-trisomic genes during development in individuals with DS (Lyle et al., 2009). It is important to define the etiology of phenotypes associated with DS, such as skeletal deficits, to identify possible mechanisms related to the development of phenotypes and possible therapeutic value.

1.1.3 Skeletal Deficits Associated with DS

The increased average expected lifespan of individuals with DS (~60 years) is mostly attributable to societal acceptance and therapeutic advancements (Baird & Sadovnick, 1989; Bittles & Glasson, 2004; Weijerman & de Winter, 2010), but individuals with DS are thus at increased risk for low bone mineral density (BMD) and fractures. Skeletal deficiencies and lack of bone mass accrual during development predispose people with Ts21 to fragility fractures, and at later ages, osteoporosis (Baptista et al., 2005; Barnhart & Connolly, 2007; Center et al., 1998; Hawli et al., 2009). Bones are significantly weaker in adults with DS as compared to others with intellectual disabilities or normally developing individuals (Geijer, Stanish, Draheim, & Dengel, 2014; Rosello, Torres, Boronat, Llobet, & Puerto, 2004; van Allen, Fung, & Jurenka, 1999); all people with DS are at risk for osteoporosis and osteopenia (de Graaf, Buckley, & Skotko, 2017; de Moraes et al., 2008; Keeling, Hansen, & Kjaer, 1997); and a high percentage of older individuals with DS have suffered fractures (van Allen et al., 1999). Spine trauma and femur fractures in this population are increasingly significant causes for morbidity (Chaney & Eyman, 2000; McKelvey et al., 2013), and the rate of falls is increased in persons with cognitive impairment (Baptista et al., 2005). Although the risk for osteoporosis is higher in adults with intellectual disabilities, the overall bone density screening rates and reports of fracture incidence are lower in these same individuals (Dreyfus, Lauer, & Wilkinson, 2014; LaCombe & Roper, 2020). Individuals with DS exhibit many hallmarks associated with osteoporosis including a lower BMD, altered geometry, and reduced overall strength. These skeletal deficits found in DS are not only age- and sex-dependent, like normally developing individuals, but are also influenced by having three copies of the genes on Hsa21. Because of the known skeletal abnormalities in all people with DS and the increasing age in the same population, there is a critical need to address the etiology of these skeletal abnormalities.

Some differences in bone properties between males and females with Ts21 have been observed, but low sample sizes, variety of analysis methods, wide array of ages, different skeletal measurement sites, and the etiology of sexual dimorphism remains unclear. Adolescent females with DS are hypothesized to acquire BMD at a lower rate compared to adolescent males with DS (Baptista et al., 2005; Gonzalez-Aguero et al., 2011). BMD is decreased in the lumbar spine of 12-16 year old males and females (analyzed together) with DS compared to age matched adolescents (Kao, Chen, Wang, & Yeh, 1992). Twenty adolescents with DS (males and females analyzed

together, average age of ~15 years) compared to 20 males and females without DS (average age of ~13 years) showed a lower BMD in lumbar spine, hip, and whole body (Matute-Llorente, Gonzalez-Aguero, Gomez-Cabello, Vicente-Rodriguez, & Casajus, 2013). However, no differences were seen in femur BMD between males and females with Ts21 in a study of 12 males and 14 females with DS (average age ~17 and 16 years, respectively) (Matute-Llorente et al., 2017). When the lumbar vertebrate of males and females (average age ~25 years) with and without DS were analyzed, males with DS as compared to controls had 25% lower BMD and females with DS had 14% lower BMD (Angelopoulou et al., 1999). Both males (average age ~26 years) and females (average age ~24 years) showed a lower BMD than control groups of males and females, and BMD was 9% lower in males with DS as compared to females with DS (Angelopoulou et al., 1999). Males with Ts21 have been reported to have greater BMD and bone area in the upper and lower limbs than females with DS (Baptista et al., 2005). Additionally, osteopenia has been reported to occur earlier in males with DS (McKelvey et al., 2013) and unlike the most common forms of osteoporosis where 80% of the affected individuals are women, osteoporosis affects both men and women with Ts21. To determine BMD, most studies use Z-scores (healthy subjects of same age and sex) (Angelopoulou et al., 2000; Costa et al., 2017) and others use T-scores (healthy subjects between 25 and 30 years of the same sex and race at peak bone mass) (Baptista et al., 2005; Carfi et al., 2017; Kao et al., 1992). Differences in calculations of BMD using T- or Z-scores to determine a low bone mass or osteoporosis add to the variation and bias in individuals with DS.

Recent publications detail skeletal deficiencies across life stages in males and females with DS in larger sample sizes and compared to normal developing populations. When femoral neck and lumbar spine was measured in 234 males and females with Ts21 ages 20-69 and compared with a reference control sample, both males and females with DS showed lower lumbar spine BMD in every decade of life measured (Carfi et al., 2017). Males with DS had reduced femoral neck BMD beginning in their 20s but females with DS did not show reduced femoral neck BMD until their 40s. Both males and females with Ts21 (237 individuals with DS aged 15-64) had reduced lumbar spine and femoral neck BMD from their 20s to their 60s as compared to a reference population (Costa et al., 2018). When 128 adults with DS (ages 18-54) were compared to 723 age-matched adults without DS and other intellectual disabilities, lumbar spine BMD in men was relatively stable in early to mid-adulthood, and bone mineral accrual was later in women than men with DS (Tang et al., 2019). Women with DS also saw a rapid loss of bone mass after age 40. Both

men and women with DS had higher rates of osteopenia and osteoporosis than a reference population. Taken together, these data indicate different skeletal deficits seen in males and females with DS, but they are complex in their nature, and not well defined in relation to age, skeletal site, and fracture risk.

1.2 Mouse Models of DS

Mouse models of DS. Human chromosome 21 is shown at the top of the figure, with mouse genome orthologous regions found Mmu16 (orange), Mmu10 (red), and Mmu17 (light green). A few known Hsa21 genes are listed below each chromosome. Ts65Dn is shown in brown and Dp1Tyb is shown in dark green.

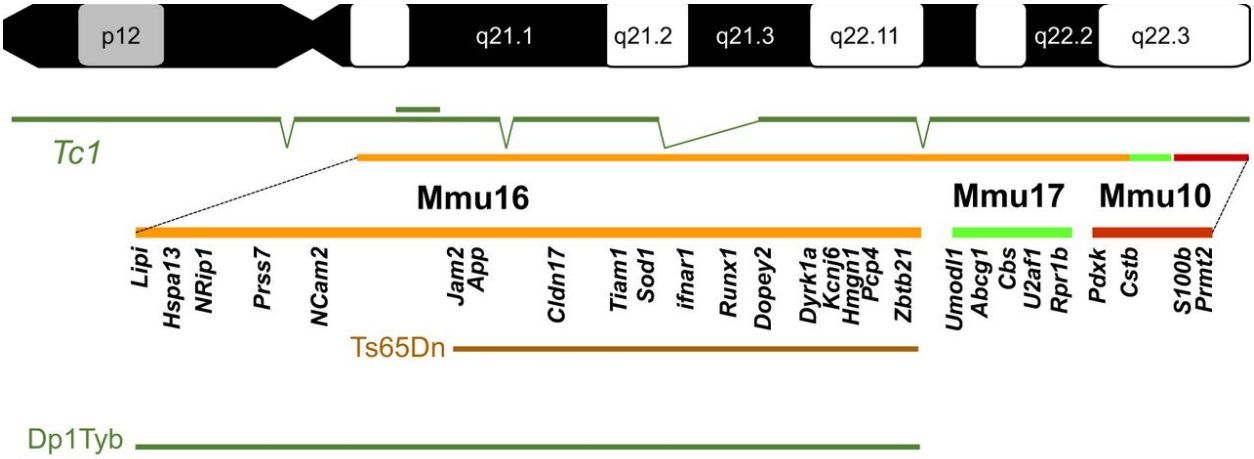

1.2.1 Ts65Dn

Mouse models recapitulate the genetic (trisomy) and phenotypic (DS-associated traits) features attributed to Ts21 and are utilized to understand skeletal phenotypes associated with DS. The Ts(17^{16})65Dn mouse (Ts65Dn), the most widely used and well-characterized mouse model of DS, has conserved homology between Hsa21 and Mmu16 (Gupta, Dhanasekaran, & Gardiner, 2016; Roper & Reeves, 2006; Sturgeon & Gardiner, 2011). Ts65Dn displays a segmental trisomy of the distal end of Mmu16 that triplicates about half of the gene orthologs found on Hsa21 (Reeves et al., 1995; Sturgeon & Gardiner, 2011). Additionally, Ts65Dn mice contain three copies of ~35 protein coding genes from mouse chromosome 17 (Mmu17) that are orthologous to Hsa6 (Duchon et al., 2011; Gupta et al., 2016; Reinholdt et al., 2011). Ts65Dn mice exhibit several phenotypes seen in humans with DS including cognitive impairment, craniofacial deficits, and cardiovascular

anomalies (Baxter, Moran, Richtsmeier, Troncoso, & Reeves, 2000; Blazek, Gaddy, Meyer, Roper, & Li, 2011; Holtzman et al., 1996; Insausti et al., 1998; Richtsmeier, Baxter, & Reeves, 2000; Williams, Mjaatvedt, & Moore, 2008). Ts65Dn mice display a reduction in BMD, osteoporotic-like structural deficiencies in the mechanical strength, cortical and trabecular bone of the femur in adolescent and adult mice (Blazek et al., 2011; Fowler et al., 2012; Parsons, Ryan, Reeves, & Richtsmeier, 2007).

Skeletal Deficits Associated with Ts65Dn Mice

Adult Ts65Dn male mice show structural and biomechanical skeletal deficits (Blazek et al., 2011; Fowler et al., 2012; Parsons et al., 2007). Ts65Dn male mice exhibit significantly less BMD, BMC and bone area in both femur and skull at 6 and 16 weeks when compared to euploid littermates (Blazek et al., 2011). A significantly lower percentage of bone volume (bone volume/tissue volume--BV/TV) was observed in trabecular bone of trisomic mice as compared to wild-type littermates. Ts65Dn male mice also exhibited significantly lower trabecular number and significantly higher trabecular separation at both time points. These changes indicate that trisomy causes altered trabecular microstructure that is more poorly organized, similar to that observed in osteoporotic bone. Cortical bone analysis of 6-week-old male mice showed significantly lower cross-sectional area and mean total periosteal perimeter in Ts65Dn as compared to control littermate mice. Mechanical parameters that assess bone strength were also significantly lower in male Ts65Dn mice as compared to euploid littermates, as seen with a reduced ultimate load and stiffness in Ts65Dn mice at 6 and 16 weeks of age. A significant increase in osteoclast surface and osteoclast number was observed in 6-week-old Ts65Dn compared to wild-type male mice (Blazek, Abeysekera, Li, & Roper, 2015). Overall, studies in mice and humans imply that trisomy causes developmental bone abnormalities, compromised bone strength, and early onset osteoporosis due to a combination of altered developmental, homeostatic and resorptive bone mechanisms (Blazek, Abeysekera, et al., 2015; Blazek et al., 2011; Fowler et al., 2012).

Although skeletal differences between normal and trisomic bone have been established using DS mouse models, little has been done to examine the skeletal structure, mechanics and cellular composition affected by trisomy and depending on sex, mostly because female Ts65Dn mice are reserved for colony maintenance. Contribution of the additional genes from Mmu17

found in trisomic Ts65Dn mice to skeletal phenotypes is unknown and requires additional research (Duchon et al., 2011; Gupta et al., 2016; Reinholdt et al., 2011).

1.3 Ts1Rhr

The occurrence of decreased BMD seen in individuals with DS has been established, however the etiology remains unknown (Olson & Mohan, 2011). It is unclear if specific genes are the causative means of reduced BMD therefore, the analysis of the skeletal phenotype in mouse models of DS can help identify mechanisms that contribute to skeletal anomalies. Ts1Rhr mice contained 33 orthologous Hsa21 genes found within the DSCR including *Dyrk1a* (Olson et al., 2004) and were generated to determine if genes found in the DSCR were sufficient to produce phenotypes seen in DS and Ts65Dn (Olson et al., 2007). Ts1Rhr were used to investigate the contribution of DSCR genes in the development of skeletal abnormalities of DS (Olson & Mohan, 2011). No differences in BMD were seen at 3 or 16 weeks in male or female Ts1Rhr mice perhaps due to the low number of genes at dosage imbalance, minimal impact of genes in three copies in this model on skeletal structure, ages sampled or the methodology used, including just examining BMD in these animals (Olson & Mohan, 2011). The use of additional skeletal analyses could reveal deficits in femoral architecture or cortical geometry that were not investigated in previous studies and elucidate novel genetic contributions associated with skeletal abnormalities seen in DS.

1.3.1 Dp1Tyb

C57BL/6J.129P2-Dp(16Lipi-Zbtb21)1TybEmcf/Nimr (Dp1Tyb) mice have a duplication on Mmu16 *Lipi* to *Zbtb21* spanning 23 Mb with 148 coding genes and contain three copies of all of the genes on Mmu16 that are orthologous to Hsa21 (Lana-Elola et al., 2016). Lana-Elola et al. investigated which genes on Hsa21cause cardiovascular defects associated with DS and how they arise. To identify dosage-sensitive critical regions and candidate genes, they generated Dp1Tyb mice. Then they produced 7 additional mouse strains that were used to identify the genetic basis of DS phenotypes and narrowed the potential genes to a list of 39 genes, and then showed at least 2 genes were required in three copies to cause heart defects (Lana-Elola et al., 2016). Also, both male and female Dp1Tyb mice are fertile which facilitates examination of skeletal features for both sexes in this mouse model. It has been hypothesized that increased dosage of one or more

genes on Hsa21 results in DS phenotypes (Delabar et al., 1993; Korenberg et al., 1994; Lyle et al., 2009). Previous mouse models have been used to identify dosage sensitive genes contributing to some DS phenotypes (Baek et al., 2009; Chakrabarti et al., 2010; Lana-Elola et al., 2016; Lana-Elola, Watson-Scales, Fisher, & Tybulewicz, 2011). The Dp1Tyb mouse model will help to identify the contribution of gene dosage from Mmu16 and skeletal deficits associated with DS.

1.4 Role of DYRK1A/*Dyrk1a* in Skeletal Anomalies Associated with DS

Skeletal phenotypes associated with DS and Ts65Dn mice are well known, however little is known about the origins of the bone phenotypes (Arron et al., 2006; Blazek, Malik, et al., 2015). Dual specificity tyrosine phosphorylation-regulated kinase 1a (*DYRK1A*), is found in three copies in humans with DS and Ts65Dn mice. It has been hypothesized that altered expression of *DYRK1A* contributes to several DS phenotypes including skeletal abnormalities (Blazek, Malik, et al., 2015). Transgenic mice that overexpress *Dyrk1a* have severe appendicular skeletal deficiencies and an osteopenic phenotype (Lee et al., 2009). DYRK1A is a known negative regulator of the key pro-osteoclastic transcription factors NFAT and RCAN1 (Lee et al., 2009). *Dyrk1a* and *Rcan1* overexpression negatively regulate *Nfat* transcriptional activity via phosphorylation of NFAT and inhibition of calcineurin by RCAN1, respectively (Arron et al., 2006; Lee et al., 2009). Phosphorylation of NFAT reduces its nuclear localization and transcriptional activity (Lee et al., 2009). NFAT has been known to be involved in the differentiation and survival of osteoblasts and osteoclasts (Lee et al., 2009). RCAN1 has been known to regulate calcineurin, which inhibits the function of NFAT, if overexpressed it can attenuate osteoclast differentiation (Arron et al., 2006).

DYRK1A is a candidate gene for skeletal abnormalities seen in humans with DS (Abeysekera et al., 2016; Blazek, Abeysekera, et al., 2015). Transgenic Ts65Dn, $Dyrk1a^{+/-}$ mice, with only two copies of *Dyrk1a* from conception onward in all tissues, rescued skeletal deficits such as femoral BMD, trabecular thickness, number, separation and percent bone volume (Blazek, Abeysekera, et al., 2015). Cortical thickness and cross-sectional area were increased to euploid levels in Ts65Dn, $Dyrk1a^{+/-}$ (Blazek, Abeysekera, et al., 2015). In addition, *Dyrk1a* copy number is associated with decreases in osteoblast number and activity and an increase osteoclast number, causing an imbalance in bone formation and resorption (Blazek, Abeysekera, et al., 2015). Ts65Dn femurs exhibit significant decreases in ultimate force, stiffness, and energy of failure when compared to

euploid littermates, however, these are rescued to euploid levels when *Dyrk1a* copy number is reduced in Ts65Dn mice (Blazek, Abeysekera, et al., 2015).

1.5 Skeletal Anatomy

The skeleton is divided into major structures axial and appendicular. Axial bone refers to bones that located on the axis of the body, including the skull and vertebral column and rib cage. The appendicular skeleton includes the pelvis, pectoral, and upper and lower extremities. Long bones, particularly the femur and humerus, are a part of the appendicular skeleton. Major architectural portions of the long bone can be divided into regions called the epiphysis (distal and proximal ends), metaphysis (region between epiphysis and diaphysis, contains the growth plate), and diaphysis (midshaft, hollow portion that contains the marrow cavity) (Burr & Allen, 2014).

1.5.1 Microstructure of Bone Organization

Organization of bone is determined by its function and mineralization. Collagen associates into fiber via triple helix conformation that is stabilized by cross-links (Burr & Akkus, 2014; Fonseca, Moreira-Goncalves, Coriolano, & Duarte, 2014; Rodan, 1992). These fibrils are then arranged into lamellar bone or sheets and can be found in the endocortical or periosteal surface and trabeculae (Burr & Akkus, 2014). Primary bone is deposited on a cartilage surface, without resorption of old bone. Secondary bone is bone that is deposited after resorption and highly organized consisting of osteons (Burr & Akkus, 2014). Primary bone is arranged as either lamellar sheets, fibrolamellar, or osteons each having mechanical or physiological properties (Burr & Akkus, 2014). Osteons refer to concentric circles that fill vascular channels (Burr & Akkus, 2014; Florencio-Silva, Sasso, Sasso-Cerri, Simoes, & Cerri, 2015). These microstructures form a larger macrostructure of bone commonly referred to as cortical (compact) and trabecular (spongy or cancellous) bone (Burr & Akkus, 2014; Florencio-Silva et al., 2015).

1.5.2 Macrostructure

The diaphysis of the long bone and the skull are classified as cortical and function to provide protection and support (Burr & Akkus, 2014). Compact bone is made of densely packed osteons that fill vascular channels with bone in concentric layers to form a haversian system (Burr

& Akkus, 2014; Rodan, 1992). In between the haversian canals are spaces, referred to as lacunae where osteocytes are found (Burr & Akkus, 2014; Rodan, 1992). Canaliculi are small channels that connect mature osteocytes to one another (Burr & Akkus, 2014).

Cancellous or spongy bone can be found in the metaphysis of long bones, the vertebrae, ribs and illac crests (Burr & Akkus, 2014; Fonseca et al., 2014). It consists of plates and rods of bone that are highly interconnected (Burr & Akkus, 2014) and this apparent haphazard arrangement provides structural support. The number, size, and organization of trabecular bone influences the mechanical strength of the bone (Wallace, 2014b). The interaction of mineralization, microstructure and macrostructure define both whole bone and material properties of bone, affecting the overall bone quality and resistance to fracture (Wallace, 2014b).

1.5.3 Background of Bone Biology

The skeleton is a highly dynamic and multifunctional organ that provides several important functions within the body, including mechanical support, protection, mineral homeostasis, and a source of hematopoiesis (Burr & Akkus, 2014). Bone is considered a hierarchical material ranging from nanostructures to macrostructures (Burr & Akkus, 2014; Wallace, 2014b). At the nanoscale level bone is comprised of mineral, collagen, and noncollangeous proteins (Burr & Akkus, 2014). These nanoscale materials then form larger composite structures of mature bone consisting of cortical bone and trabecular bone each with distinct architecture (Rodan, 1992). Hierarchical arrangement of bone allows for it to perform several functions including support, mechanical strength, adaption to loads, and repair of damaged skeletal tissue all dependent on the composition of the skeleton (Burr & Akkus, 2014).

The cells that support bone formation and homeostasis are osteoblasts, osteoclasts, and osteocytes (Bellido, Plotkin, & Bruzzaniti, 2013; Burr & Akkus, 2014). These cells are responsible for creating the lamellar structure of bone to form the macrostructure of bone (Burr & Akkus, 2014). To fulfill its functions as well as to form the skeleton, bone is continually formed and resorbed via osteoblasts and osteoclasts, otherwise known as bone remodeling (Burr & Allen, 2014; Florencio-Silva et al., 2015; Rodan, 1992). Bone remodeling consists of resorption followed by bone formation at the same location and its serves to renew the skeleton (Burr & Allen, 2014; Rodan, 1992). Bone modeling refers to either the formation or resorption of bone at a given surface (globally independent) and serves to maintain bone shape and size (Burr & Allen, 2014). Bone

homeostasis is often referred to the coupling activity of osteoblasts and osteoclasts in effort to maintain skeletal integrity and mineral homeostasis (Burr & Allen, 2014; Rodan, 1998). Bone mineralization, structure, and mechanical strength are achieved by the coordination of osteoclastic resorption and osteoblastic formation (Rodan, 1998). The coordination or coupling activity is thought to maintain bone balance, meaning equal amount of bone that is resorbed an equal amount of bone is formed at a specific location (Burr & Allen, 2014). Normally the balance is slightly negative meaning slightly less bone is replaced than is resorbed (Burr & Allen, 2014; Rodan, 1998). An imbalance in this process can lead to disease states such as osteoporosis, a net loss in bone mass and therefore causes an increase in fracture risk.

1.5.4 Bone Composition

The extra cellular matrix of bone consists of mineral, organic polymers, and water (Burr & Akkus, 2014; Florencio-Silva et al., 2015). Calcium hydroxyapatite crystal, ($Ca^{10}(PO^4)^6(OH)^2$) is the major mineral found in bone, and makes up about 50-70% of mature bone (Burr & Akkus, 2014; Florencio-Silva et al., 2015). The organic portion of bone is made of approximately 90% type 1 collagen and about 10% is made of noncollagenous proteins (NCPs). Collagen forms fibrils that are arranged into lamellar sheets, and then connected by cross-links that influence the mechanical properties of the bone (Burr & Akkus, 2014; Burr & Allen, 2014). NCPs play a role in the regulation of collagen formation, mineralizing, cell attachment, fibril size and microcrack resistance (Burr & Akkus, 2014). The composition of bone can determine its ability to resist fracture, commonly referred to as bone quality. Bone quality is determined by architecture and geometry, material properties, bone turnover, microdamage, and response to mechanical stimuli (Burr & Akkus, 2014; Fonseca et al., 2014).

1.6 Function of Bone Cells

The skeleton is a dynamic organ constantly undergoing resorption followed by formation, allowing the bone to alter its structure or provide minerals to the rest of the body (Florencio-Silva et al., 2015; Fonseca et al., 2014; Robling, Fuchs, & Burr, 2014). Bone growth, modeling and remodeling are regulated by spatial and temporal relation between resorption and formation. (Bellido et al., 2013; Burr & Allen, 2014; Fonseca et al., 2014; Robling et al., 2014). This process

is thought to contribute to mineral homeostasis and mechanical strength (Robling et al., 2014; Rodan, 1992).

1.6.1 Osteoblasts

Osteoblasts are cuboidal cells and their main function is to synthesize new bone matrix (Florencio-Silva et al., 2015; Rodan, 1992, 1998). Osteoblasts are normally found on the surface of the bone and form the osteoid that consists of type 1 collagen and other matrix proteins (Florencio-Silva et al., 2015; Rodan, 1992, 1998). Mineralization of the newly formed bone matrix is accomplished via alkaline phosphatase (ALP) and osteocalcin activity (Florencio-Silva et al., 2015; Rodan, 1992). As osteoblasts deposit new bone matrix they can become trapped and differentiate into osteocytes or become quiescent as bone lining cells (Bonewald, 2011; Florencio-Silva et al., 2015; Rodan, 1992). Osteoblasts are derived from the mesenchymal stem cell lineage (Bellido et al., 2013; Florencio-Silva et al., 2015; Rodan, 1992) and their differentiation is regulated by an array of transcription factors and hormonal signaling including BMPs, TGF-B, PTH, and Wnt signaling (Bellido et al., 2013; Florencio-Silva et al., 2015). The expression of *Runx2 and Osterix* (*Osx*) are critical in osteoblast differentiation (Bellido et al., 2013; Florencio-Silva et al., 2015; Nakashima et al., 2002). *Runx2*, the master regulator of osteoblast differentiation, is required for commitment to the osteoblast lineage and for subsequent *Osx* expression (Bellido et al., 2013; Nakashima et al., 2002; Wysokinski, Pawlowska, & Blasiak, 2015). Changes in osteoblast differentiation and/or activity can increase bone mass and reduce fracture risk (Burr & Allen, 2014; Fonseca et al., 2014; Rodan, 1998).

1.6.2 Osteoclasts

Osteoclasts are large multinucleated cells and are the primary resorptive cells in the bone (Florencio-Silva et al., 2015; Rodan, 1992). They are essential for bone remodeling and modeling by maintaining homeostasis and reshaping bone in response to mechanical stress (Bellido et al., 2013; Rodan, 1992). They are derived from the hematopoietic monocyte-macrophage lineage in the bone marrow (Bellido et al., 2013; Florencio-Silva et al., 2015). Osteoclast precursors are stimulated by M-CSF and Receptor activator of nuclear factor kappa-B ligand (RANKL) which are secreted by osteoblasts and osteocytes (Bellido et al., 2013; Florencio-Silva et al., 2015).

RANKL is required for the differentiation of mature osteoclasts by promoting fusion with other osteoclast precursors, acquisition of biomarkers specific to osteoclasts and stimulation of resorption (Bellido et al., 2013; Florencio-Silva et al., 2015). OPG is a decoy receptor of RANKL, inhibits osteoclastogenesis, and is mainly produced by osteocytes and osteoblasts (Bellido et al., 2013; Bonewald, 2011; Florencio-Silva et al., 2015; Ono & Nakashima, 2018). RANKL induces the NFATc1 pathway which essential for osteoclastogenesis and its upregulation increases osteoclastic resorption (Bellido et al., 2013; Bonewald, 2011; Lee et al., 2009; Ono & Nakashima, 2018; Zhou et al., 2010). Fusion of osteoclasts is required for maturation and resorptive activity and requires at least 3 or more nuclei to characterize active mature osteoclasts (Bellido et al., 2013). When osteoclasts are recruited to the bone surface to initiate resorption, they first attach to the bone surface and then create a sealing zone to acidify and degrade the bone mineral matrix through the action of cathepsin K and matrix metalloproteases (Bellido et al., 2013; Florencio-Silva et al., 2015). Abnormal increases osteoclast formation and activity can lead to increases in resorption that exceed the rate of bone formation (Bellido et al., 2013; Burr & Allen, 2014).

1.6.3 Osteocytes

Osteocytes are the major cells found within bone and are the longest lived (Florencio-Silva et al., 2015). Osteocytes are mature osteoblasts that were embedded in newly formed osteoid (Bonewald, 2011; Florencio-Silva et al., 2015). They are located within the lacunae of the bone and have dendrites that extend outwards that connect to other osteocytes (Florencio-Silva et al., 2015; Rodan, 1992) creating a lacunocanalicular network. Osteocytes are thought to aid in signal transduction by sensing mechanical strain and converting it into biochemical signals (Florencio-Silva et al., 2015; Robling et al., 2014). Detection of shear stress activates osteocytes to release paracrine factors between other osteocytes to coordinate the activities of osteoblasts and osteoclasts (Bellido et al., 2013; Plotkin & Bivi, 2014b). Response to mechanical stimuli allows the bone to adapt to mechanical loads and osteocytes are thought to mediate this response by regulation of the remodeling process (Burr & Allen, 2014; Robling et al., 2014; Wallace, 2014b).

1.6.4 Bone Formation

There are two types of bone formation: endochondral and intramembranous ossification (Burr & Allen, 2014; Nakashima et al., 2002; Sinha & Zhou, 2013). Endochondral ossification starts with the production of a hyaline cartilage template by chondrocytes that later become calcified osteoprogenitor cells. Then the cartilaginous template is replaced by mineralized bone tissue (Burr & Allen, 2014; Nakashima et al., 2002; Sinha & Zhou, 2013). Long bones such as the femur and tibia, and bones found at the base of the skull are formed by endochondral ossification. Intramembranous ossification does not require a cartilage template, comprises of flat bones in the skull, the mandible and clavicles. Mesenchymal cells condense and differentiate directly into osteoblasts to produce bone matrix (Burr & Allen, 2014; Nakashima et al., 2002; Sinha & Zhou, 2013). The skull, scapula and clavicle are some of the bones formed via intramembranous ossification.

1.6.5 Bone Modeling and Remodeling

Bone modeling is formation of bone on an already existing bone surface most prominent during longitudinal growth and development (Burr & Allen, 2014; Seeman, 2008). Modeling is the primary function to increase bone mass and maintain bone size and shape (Burr & Allen, 2014; Seeman, 2008). Mechanical strain is the main signal for modeling and activates the recruitment of either osteoblast or osteoclasts (Burr & Allen, 2014; Robling et al., 2014; Seeman, 2008). The purpose of modeling during growth is to reach skeletal maturity, or peak bone mass, and this process declines in adulthood (Burr & Allen, 2014; Seeman, 2008; Seeman & Delmas, 2006).

Bone turnover is the coordinated activity of osteoclast bone resorption followed by osteoblast bone formation at the same skeletal site (Burr & Allen, 2014; Rodan, 1992, 1998). The activity between osteoblasts and osteoclasts must be balanced to prevent bone loss or excess bone formation (Burr & Allen, 2014; Rodan, 1992, 1998; Seeman, 2008). Remodeling is the process in which bone matrix is replaced in response to microdamage or osteocyte apoptosis (Burr & Allen, 2014; Seeman, 2008). Bone turnover becomes less rapid after epiphyseal plate closure and peak mechanical strength is achieved. The activity of remodeling after the growth period gives the bone the ability to adapt and respond to mechanical stress (Burr & Allen, 2014; Fonseca et al., 2014; Robling et al., 2014; Seeman, 2008). The frequency of remodeling is high during growth to adapt

to stresses (Seeman & Delmas, 2006). Factors thought to regulate remodeling include RANKL, OPG, IGF-1, TGF-B, hormones, cytokines and Wnt (Burr & Allen, 2014; Plotkin & Bivi, 2014a; Rodan, 1992; Seeman, 2008). The rate of turnover is influence by age, genetics, physical activity, nutrition and hormonal activity (Burr & Allen, 2014).

1.7 Fundamentals of Skeletal Biomechanics

Bone is considered a hierarchical material having various layers of structural organization at different scales that perform a variety of functions (Berman, Clauser, Wunderlin, Hammond, & Wallace, 2015; Rho, Kuhn-Spearing, & Zioupos, 1998; Wallace, 2014a). To assess the mechanical strength of the bone or resistance to fracture, mechanical tests such as three-point bending is performed (Cole & van der Meulen, 2011). When a load is applied in a monotonic manner, deformation occurs and when that load exceeds the strength of the bone fracture will occur (Cole & van der Meulen, 2011; Martin, 2015; Wallace, 2014a). As load or force is used as a function of deformation or displacement, the force-displacement curve is produced (Turner & Burr, 1993; Wallace, 2014a). The force-displacement curve can be divided into three regions: an initial linear (elastic) region, a postyield (plastic) nonlinear region that contains ultimate load, and the failure point in which catastrophic failure occurs (Cole & van der Meulen, 2011; Martin, 2015; Wallace, 2014a). In the elastic region the bone is deformed as the load increases; if the load is removed, the bone can return to its original shape (Cole & van der Meulen, 2011; Martin, 2015; Wallace, 2014a). The slope of the elastic region is related to structural stiffness (Turner & Burr, 1993; Wallace, 2014a). If the load increases past the linear region known as the yield point, permanent (plastic) deformation will occur and the bone will not return to its original shape if the load is removed (Cole & van der Meulen, 2011; Martin, 2015; Wallace, 2014a). The plastic region, which contains ultimate force or load, is defined as the structural strength before catastrophic failure (Martin, 2015; Wallace, 2014a). Finally the area under the curve is a measure of work, or energy absorbed by the bone until fracture occurs (Martin, 2015; Wallace, 2014a).

Whole bone strength or mechanical properties depend on the geometry, size of the bone, and material properties (Cole & van der Meulen, 2011; Wallace, 2014a). Normalizing for shape and size, the load displacement curve is converted to stress (force/area) – strain (Δlength/initial length) and information related to tissue level properties that excludes geometric properties is obtained (Cole & van der Meulen, 2011; Wallace, 2014a). The slope of the stress-strain curve is intrinsic

stiffness, modulus, yield stress, ultimate stress, and toughness (area under the curve); measures that are similar to the load-displacement curve but only accounting for tissue level material properties (Cole & van der Meulen, 2011; Martin, 2015; Wallace, 2014a).

1.8 OSTERIX/*Sp7* as an Osteoblast Transcription Factor and its Role in Bone Growth

The appendicular and axial skeleton are derived from distinct cell linages from the paraxial mesoderm and the lateral plate mesoderm (Rodda & McMahon, 2006). Several lineages that contribute to the development of the skeleton, each contribute to generation of the bone matrix secreting cell type, the osteoblast (Rodda & McMahon, 2006). OSTERIX/SP7(OSX*)* is a zinc finger family transcriptional factor critical for osteoblast differentiation and endochondral bone formation (Chen et al., 2014; Huang & Olsen, 2015). The gene for *Osx* is highly conserved between mice and humans and it is located on Mmu15 and Hsa12, respectively, and there are only 2 exons (Zhang, 2012). OSX activation is downstream of RUNX2 and required for osteoblast maturation. It is necessary for embryonic skeletal development and postnatal growth (Zhang, 2012). Both endochondral and intramembranous ossification require osteoblasts that express OSX (Nakashima et al., 2002; Rodda & McMahon, 2006).

Osx1-GFP::Cre (*Osx*-Cre), a BAC transgenic mouse line expressing a GFP::Cre fusion protein from the regulatory sequence of *Osx*, was generated to direct gene deletion in the osteoblast lineage (Rodda & McMahon, 2006). The Cre activity is normally confined to the osteogenic perichondrium, periosteum and osteoblast lineage cells within the marrow cavity (Rodda & McMahon, 2006). OSX is required for osteoblast differentiation, function, and bone formation and can be used to understand skeletogenesis at specific stages of bone development (Huang & Olsen, 2015).

1.9 Thesis Hypotheses

1.9.1 Hypothesis 1: Sexual Dimorphism in the Dp1Tyb Mouse Model of DS

Gene dosage influences skeletal abnormalities and sexual dimorphism contributes to differences seen between humans (male and female) with DS. Thus, we examined male and female control and Dp1Tyb animals. Our hypothesis was that Dp1Tyb male mice would exhibit similar phenotypes compared to male individuals with DS, while female mice would display a distinct

skeletal phenotype compared to their male littermates. The onset and severity of skeletal deficits, such as osteoporosis, are also influenced by age. Hence, we hypothesized that skeletal deficits are differentially affected depending on chronological age in Dp1Tyb animals with increasing severity in older mice.

1.9.2 Hypothesis 2: Role of *Dyrk1a* in Bone Abnormalities in Ts65Dn/*Dyrk1a*$^{fl/+}$/*Osx*-Cre^{+} Mice

Dyrk1a is found in three copies in humans with DS and Ts65Dn animals, and contributes to skeletal abnormalities. In trisomic Ts65Dn adolescent mice, *Dyrk1a* copy number has been shown to increase osteoblast number, however osteoclast number is decreased in adult trisomic animals (Blazek, Abeysekera, et al., 2015; Fowler et al., 2012). Altered expression of *Dyrk1a* results in skeletal deficits associated with a low bone turnover phenotype, causing deficits in skeletal microarchitecture and material properties. We hypothesize that reduction of *Dyrk1a* to two copies in mature osteoblasts in an otherwise trisomic mouse will ameliorate skeletal deficits associated with bone formation. An *Osx*-cre driver was used to genetically return *Dyrk1a* to normal levels in the preosteoblasts and mature osteoblasts of male and female *Osx*-Cre,Ts65Dn,*Dyrk1a*$^{fl/+}$ mice in order to understand trisomic *Dyrk1a's* role in osteoblast differentiation, function, and survival.

CHAPTER 2. MATERIALS AND METHODS

2.1 Experimental Animals

C57BL/6J.129P2-Dp(16Lipi-Zbtb21)1TybEmcf/Nimr (Dp1Tyb) mice (Lana-Elola et al., 2016) were bred at the Medical Research Council (MRC) Harwell Institute, UK by crossing to C57BL/6J mice. Genotyping was undertaken using custom probes (Transnetyx). Female mice were nulliparous. Femurs were isolated from Dp1Tyb and littermate wild-type mice at 6 and 16 weeks of age. Right femurs were stored in phosphate buffered saline (PBS)-soaked gauze, shipped on dry ice and stored at -80º C to be used for microcomputed tomography (μCT) analysis and mechanical testing. Left femurs were stored in 70% ethanol and analyzed for dynamic and static histomorphometry. From our previous skeletal analyses, we estimated that we would need ten mice of each genotype to quantify both trabecular and cortical bone parameters ($\alpha = 0.05$, $1- \beta = 0.80$ in power analyses). Femurs from 6-week-old male (n=10 control, n=10 Dp1Tyb) and female (n=12 control, n=11 Dp1Tyb); and 16-week-old male (n=13 control, n=12 Dp1Tyb) and female (n=19 control, n=22 Dp1Tyb) were used. All assessment of femurs was done with investigators blind to sample genotype. Histomorphometry was only completed on 16-week-old male and female mice. All regulated procedures were carried out with approval from a Local Ethical Review Panel and under authority of a Project License granted by the UK Home Office, and in accordance with EU Directive 2010/63/EU.

2.1.1 Breeding Scheme of Ts65Dn,*Dyrk1a*$^{fl/+}$, *Osx*-Cre+ Animals

Female Ts65Dn mice with a floxed *Dyrk1a* gene (Ts65Dn, *Dyrk1a*$^{fl/+}$) were bred to *Osx1*-GFP::Cre mice$^{+/+}$ (B6.Cg-Tg(Sp7-tTA,tetO-EGFP/cre)1Amc/J). *Osx1*-GFP::Cre (*Osx*-Cre) mice are commonly used to target osteoblasts. They have a tTA and tetracycline responsive element-controlled GFP/Cre fusion protein under the control of the *Osterix (Sp7)* promoter. *Osx*-Cre is normally expressed from embryonic development E14.5 and postnatal development (Rodda & McMahon, 2006; Wang, Mishina, & Liu, 2015). All mice were generated on a ~50% B6 and 50% C3H background to match the background of Ts65Dn mice. *Dyrk1a* inducible knockdown mice (*Dyrk1a*$^{fl/+}$) were heterozygous for a construct with lox sites, that, with induced *Cre* expression, will splice out exons 5 and 6 eliminating the kinase activity of one copy of *Dyrk1a* (Fotaki et al.,

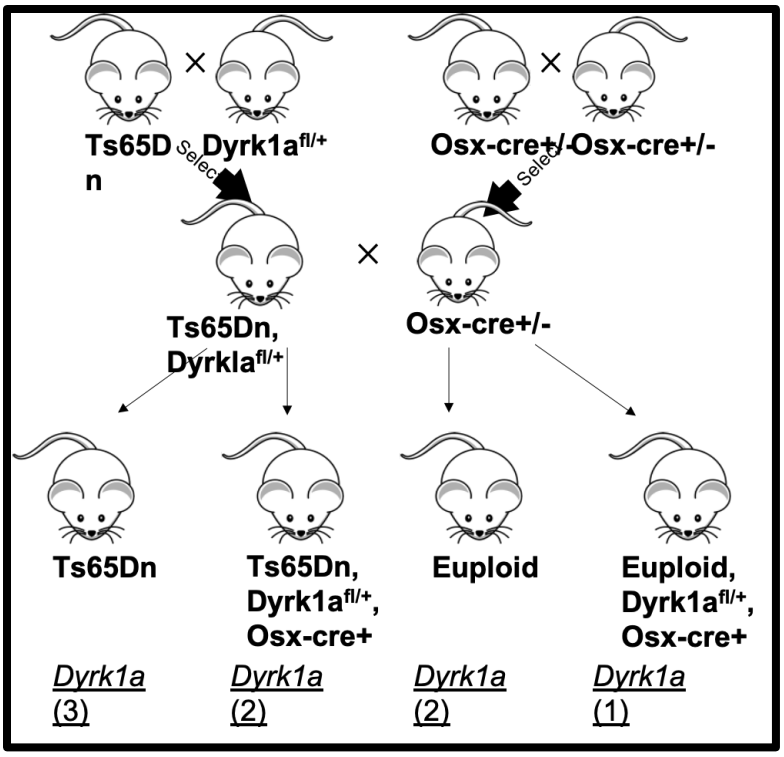

2002; Thompson et al., 2015). We have not been able to generate Ts65Dn, *Dyrk1a*$^{fl/fl}$ mice due to possible lethality of homozygous floxed offspring interacting with the trisomic genome.

Osx-Cre mice were bred to homozygosity via test cross and verification by PCR genotyping, and with 25% of the offspring containing Cre on both alleles. In Ts65Dn, *Dyrk1a*$^{fl/+}$ offspring with *Osx*-Cre transgene, active Cre recombinase will eliminate one functional copy of *Dyrk1a* in osteoblasts. Treatment with doxycycline can prevent the expression of the GFP-Cre protein and recombination of the target gene (Rodda & McMahon, 2006; Wang et al., 2015). Expected ratios of the four genotypes are: 1/8 Ts65Dn, *Dyrk1a*$^{fl/+,}$ *Osx*-Cre+; 1/8 Euploid, *Dyrk1a*$^{fl/+,}$ *Osx*-Cre+; 3/8 Ts65Dn control; 3/8 euploid control mice.

Groups of female mice were generated for testing: 3 copies of *Dyrk1a* (Ts65Dn,*Dyrk1a*$^{+/+/+}$ [same as Ts65Dn]) n=42; trisomic mice with 2 active copies of *Dyrk1a* (Ts65Dn,*Dyrk1a*$^{+/+/-}$ [same as *Dyrk1a*$^{fl/+}$,*Osx*-Cre+]) n=24; euploid mice with 2 copies of *Dyrk1a* (Eu,*Dyrk1a*$^{+/+}$) n=10; euploid mice with 1 active copy of *Dyrk1a* (Eu,*Dyrk1a*$^{+/-}$[same as *Dyrk1a*$^{fl/+}$, *Osx*-Cre+) n=7. Right femurs were stored in 70% EtOH and used for histomorphometry. Left femurs were stored in gauzed soaked PBS and used for microCT analysis and mechanical testing. To test the hypothesis that *Dyrk1a* reduction can improve the overall strength of trisomic bones and ameliorate the sexual dimorphism associated with *Dyrk1a* expression.

2.2 Genotyping

All Ts65Dn mice were genotyped using the breakpoint PCR protocol (Reinholdt et al., 2011). Ts65Dn mice carry a translocation between chromosomes (Chrs) 16 and 17 (Davisson et al., 1993). The translocation chromosome, Mmu17^{16}, is freely segregating. It carries 13.4Mb of the distal

Mmu16 fused with the centromere of Mmu17. Primers spanning the translocation breakpoint were used to genotype euploid and trisomic mice (Reinholdt et al., 2011).

The primer sequences were Chr17fwd (GTGGCAAGAGACTCAAATTCAAC) and Chr16revs (TGGCTTATTATTATCAGGGCATTT) to amplify a ~275bp product at the breakpoint sequence. A positive internal control primer set consisted of IMR8545 (TGTCTGAAGGGCAATGACTG) and IMR8546 (GCTGATCCGTGGCATCTATT) that yields a product around 544bp. The final PCR mix contained MyTaq reaction buffer (1x), MyTaq polymerase (2.5U/ul), water, mutant primers (0.5uM), internal positive control (0.4uM), and DNA (~100ng/rxn). PCR cycling conditions were for 35 cycles (94°C for 2 minutes and 30 seconds; 94°C for 15 seconds; 58.5°C for 15 seconds; 72°C for 10 seconds; 72°C for 1 minute). Products were run on an 1.5% agarose gel with 4ul of SYBRGold. The size of the PCR products was compared to DNA ladder to confirm the presence of the Ts65Dn breakpoint fragment from euploid animals.

Primer sequences for *Osx*-Cre were 30295 forward (GAGAATAGGAACTTCGGAATAGTAAC) and 30296 reverse (CCCTGGAAGTGACTAGCATTG) that amplifies a 198bp band. PCR cycling conditions was (2 minutes at 94°C, 15 seconds at 94°C, 15 seconds at 55°C, 15 seconds at 72°C, 2 minutes at 72°C) for 35 cycles with 10 minutes 4°C hold. These primers were changed to forward Osx10 (CTCTTCATGAGGAGGACCCT) and reverse TGCK (GCCAGGCAGGTGCCTGGACAT) with a ~500bp product, PCR conditions (1 minute at 94°C, 30 seconds at 94°C, 30 seconds at 55°C, 30 seconds at 68°C, 2 minutes at 72°C) for 39 cycles. Internal controls were consistent throughout the study and were 25775 forward (AGAGAGCTCCCCTCAATTATGT) and 25776 reverse (AGCCACTTCTAGCACAAAGAACT) creating a product about 253bp. Lastly, all Ts65Dn, *Dyrk1a*, *Osx*-Cre offspring underwent PCR protocol to detect the presence of the loxP sites flanking exons 5 and 6 of Dyrk1a (Thompson et al., 2015). The forward primer was 25066 (TACCTGGAGAAGAGGGCAAG) and the reverse 25067 (GGCATAACTTGCATACAGTGG) for 35 cycles (3 minutes at 95°C, 20 seconds at 95°C, 20 seconds at 60°C, 15 seconds at 72°C, 1 minutes at 72°C). WT animals produced a single band around 503bp, heterozygous animals produced amplicons at 503 and 603bp, and homozygous animals produced a single fragment at 603bp.

2.3 Fluorescent Labeling

Male and female *Osx*-Cre animals were aged to 6 weeks. Mice were injected intraperitoneally at 5 weeks of age with 0.2ml of 1.0% of Calcein green dye. Four days after initial injection of Calcein green, mice were injected again. Three days after the second injection mice were euthanized and weighed. Right femurs were extracted and used for tissue histomorphometry.

2.4 Microcomputed Tomography (uCT)

Femurs were thawed to room temperature and scanned using high-resolution μCT system, SkyScan 1172 microCT (SkyScan, Kontich, Belgium) using the following parameters: voltage 60kV, resolution 12μM, binning mode 2k and filter Al 0.5mm. Calibrations were performed daily using two cylindrical hydroxyapatite phantoms (0.25 and 0.75g/cm^3 calcium hydroxyapatite). Femurs were rewrapped in PBS soaked gauze and stored at -80ºC until mechanical testing. Reconstruction analysis was performed using NRecon and CTan software (Skyscan, Bruker microCT, Belgium). Trabecular microarchitecture and cortical geometry were accomplished using previously published protocol (Abeysekera et al., 2016; Berman et al., 2015).

Trabecular analysis was performed on the distal metaphysis with a region of interest (ROI) defined as 10% of the total bone length, approximately 1mm proximal to the distal growth plate and then extending proximally. The ROI was auto-segmented using custom Matlab (MathWorks, Inc. Natick, MA) code (Berman et al., 2015). Measurements from trabecular architecture (bone volume fraction [BV/TV], trabecular thickness, number and separation), bone mineral density (BMD) and tissue mineral density (TMD) were obtained using CTAn.

Cortical analysis was performed at a standard site 60% of the total bone length away from the distal growth plate. Seven transverse slices were generated from the standard site and cortical geometric properties were obtained from using a custom Matlab code.

2.5 Mechanical Testing

The mechanical properties of the femur were determined by 3-point bending using a mechanical testing machine (TA ElectroForce 3200; Eden Prairie, MN, USA). The femurs were thawed to room temperature and tested in the anterior-posterior direction with the posterior surface in compression (7 mm support span). The load was applied to the midpoint of each bone. The

femur was preloaded using 0.5N to establish contact with the bone and then monotonically tested to failure at a displacement rate of 0.025 mm/s while fully hydrated. Load and deflection were recorded, from which structural strength (yield and ultimate), stiffness (slope of the linear portion of the force versus displacement curve), and deformation (yield deformation, postyield deformation and total deformation) were determined (Wallace, Golcuk, Morris, & Kohn, 2009; Wallace et al., 2006). Distance from the proximal end of the femur to the location of the fracture initiation was measured using calipers. Seven transverse slices were obtained from μCT at the location of fracture and calculated geometric properties (bending moment of inertia and distance from the centroid to the tensile surface of the bone). Along with the deflection data, the moment of inertia and distance from the centroid to the tensile surface of the bone in tension derived were used to map load-displacement into stress vs. strain curves using standard equations derived from Euler-Bernoulli beam theory to estimate tissue level properties (Wallace et al., 2009). The mechanical strength, stiffness, and work/toughness were determined from the force vs. displacement and stress vs. strain curve.

$$Stress = \sigma = \frac{Fac}{2I_{AP}}(MPa)$$

$$Microstrain = \mu\varepsilon = \frac{6cd}{a(3L - 4a)} \times 10^6$$

In these equations, F is the force, d is the displacement, a is the distance from the support to the inner loading point (4 mm), and L is the span between the outer supports (7 mm). The yield point was calculated using the 0.2% offset method based on the stress-strain curve. The modulus of elasticity was calculated as the slope of the linear portion of the stress-strain curve.

2.6 Histology

Femurs were removed and placed in 70% ethanol (EtOH) and stored at room temperature until ready for use. The femur was separated from at the midshaft and the proximal and distal femurs were processed, cut and sectioned as described (Blazek et al., 2011). Briefly, right femurs were dehydrated in graded levels of EtOH, cleared in xylene and embedded in methyl methacrylate.

For dynamic histology, the midshaft of the femur was sectioned into 500μm transverse sections and ground to 40μm and then mounted using Eukitt to enhance viewing of fluorescent label. One section was read using a D-FL Epi-Fluorescence attachment on a Nikon Eclipse 80i DIC microscope, and images were taken using a Nikon DS-Fi1 digital sight camera.

2.6.1 Dynamic Histomorphometry

Mineralizing surface/bone surface (MS/BS) was assessed by measuring the double label surface (dL.S), single label surface (sL.S), and total bone surface (BS) using BioQuant software (R & M Biometrics, Nashville, TN; MS/BS = (dL.S.+ 0.5*sL.S)/BS). Mineral apposition rate (MAR) was determined by measuring the average interlabel width between two fluorochrome labels using the Bioquant software, divided by the number of days between label administration. MS/BS and MAR were used to quantify bone formation rate (BFR). BFR = MS/BS * MAR * 365; $\mu m^3/\mu m^2$/year. Based on the measurements obtained from dynamic labeling, some mice had to be removed from analysis, for the periosteal surface 16-week-old male (n=9 wild-type, n=7 Dp1Tyb) and female (n=9 wild-type, n=9 Dp1Tyb) were used. For the endocortical surface, 16-week-old male (n=10 wild-type, n=8 trisomic) and female (n=11 wild-type, n=10 trisomic) were used.

2.6.2 Static Histomorphometry

Briefly, sections of the distal femur were deplasticsized in acetone and stained for the osteoid using the Von Kossa-MacNeal's tetrachrome protocol or osteoclasts using TRAP staining. Osteoid surface/bone surface (OS/BS) was quantified using Bioquant software. For osteoclasts, osteoclast surface to bone surface (OcS/BS), and osteoclast number per 1mm tissue (Oc#/BS) were quantified using Bioquant software. 16-week-old male (n=13 control, n=10 Dp1Tyb) and female (n=11 control, n=12 Dp1Tyb) were used.

2.7 Statistical Analysis

MicroCT and mechanical testing data were analyzed using a custom Matlab code (Berman et al., 2015). For microCT, mechanical testing, and histomorphometry data, normality and homogeneity were assessed for each phenotype and any violations were transformed to achieve normality. To control for the analysis of multiple dependent variables, separate MANOVAs (Wilks'

Lambda, IBM SPSS version 26) were performed on the 6- and 16-week-old mice for trabecular (4 parameters), cortical (14 parameters) and mechanical (16 parameters) data. If the MANOVA for a given age and bone type yielded significant main or interactive effects of genotype and/or sex, follow-up 2-way factorial ANOVAs were performed on each individual parameter to identify which of the individual parameters expressed the main (or interactive) effects that were significant in the MANOVA. If the MANOVA yielded no significant effects, no additional follow-up analyses were performed. Effect sizes were obtained from the SPSS calculations of partial eta squared in each ANOVA. For each parameter with a significant interaction, posthoc analyses (Tukey's multiple comparisons test) determined differences between groups.

CHAPTER 3. RESULTS

INTERACTION OF SEXUAL DIMORPHISM AND GENE DOSAGE IMBALANCE IN SKELETAL DEFICITS ASSOCIATED WITH DOWN SYNDROME

3.1 Preface

The results for this study have been recently published in *Bone*. I was the first author for this article. I contributed to the study design, microCT analysis, mechanical testing and histological analysis. I was also responsible for writing, editing, and proofing the manuscript, and making necessary changes requested by reviewers.

Thomas JR, LaCombe J, Long R, Lana-Elola E, Watson-Scales S, Wallace JM, Fisher EMC, Tybulewicz VLJ, Roper RJ.

Bone. 2020 Apr 16:115367. doi: 10.1016/j.bone.2020.115367. [Epub ahead of print]

PMID: 32305495

3.1.1 Preliminary Skeletal Analyses

Preliminary analyses on mice at 14 weeks showed an effect of both sex ($p<0.001$) and genotype (trisomy or extra gene dosage) on the length from nose to base of tail ($p=0.001$) (Dp1Tyb male = 89.84 (SE±0.86) mm; control male = 93.12 (0.94) mm; Dp1Tyb female = 85.24 (1.15) mm; control female = 88.56 (0.41) mm; n=10 for all samples). Male and control mice overall showed a longer body at 14 weeks. The length of the femur was greater in wild-type mice as compared to Dp1Tyb mice at 14 weeks ($p<0.001$) (Dp1Tyb male = 14.78 (0.20) mm; control male = 15.72 (0.20) mm; Dp1Tyb female = 14.76 (0.22); control female = 15.40 (0.18); n=10 for all samples).

3.2 Interaction of Sex and Genotype in Dp1Tyb Mice Alters BV/TV during Skeletal Maturation

The interaction of sex (male vs. female) and genotype (three copy vs. normal copy number) was important in percent bone volume (bone volume/tissue volume or BV/TV) at both 6 and 16 weeks of age. At 6 weeks of age during longitudinal bone growth, BV/TV was reduced in male Dp1Tyb, female Dp1Tyb and female control animals as compared to male control animals (**Fig. 1A**). At 16 weeks of age, a time of skeletal maturity, BV/TV continued to be reduced in male Dp1Tyb, female Dp1Tyb and female control animals as compared to male control animals. Additionally, female Dp1Tyb mice had reduced BV/TV as compared to male Dp1Tyb mice (**Fig. 1A**). BV/TV increased in male mice from 6 to 16 weeks of age ($p<0.001$), but female mice exhibited a loss in BV/TV during the same time period ($p=0.025$). Similar data were observed for BMD in the trabecular compartment at both 6 and 16 weeks.

3.3 Interaction Between Sex and Genotype Affects Trabecular Microarchitecture in Male and Female Dp1Tyb and Wild-Type mice

Measurements of other trabecular skeletal parameters provide insight into the interaction between sex and genotype. Trabecular number (Tb.N) is increased in male wild-type mice compared to female Dp1Tyb and wild-type mice at 6 and 16 weeks (**Fig. 1B**) and trabecular thickness (Tb.Th) is greater in male wild-type mice than male and female Dp1Tyb and wild-type mice at both 6 and 16 weeks (**Fig. 1C**). Trabecular separation (Tb.Sp) is greater in female than male mice at 16 weeks (**Fig. 1D**). In male mice, Tb.N increased ($p=0.013$) and Tb.Sp decreased ($p=0.034$) from 6 to 16 weeks for both genotypes. Tb.Th showed an age × genotype interaction ($p=0.021$) in male mice. When only female mice were analyzed together at 6 and 16 weeks, Tb.N decreased and Tb.Th and Tb.Sp increased ($p<0.001$ for all).

3.4 Cortical Bone Parameters Exhibit an Interaction Between Sex and Genotype in Dp1Tyb and Control mice, with most Interactive Effects at 16 Weeks

Six week-old control male and female mice had a greater total cross-sectional area (total CSA) in the cortical bone than Dp1Tyb male and female mice (**Fig. 2A**). Total CSA increased from 6 to 16 weeks in male ($p<0.001$) but not female ($p=0.61$) mice. At 16 weeks of age, total

CSA is larger in control male than all other mice, male Dp1Tyb as compared to female Dp1Tyb mice, and female control as compared to female Dp1Tyb mice.

The sexual dimorphism and effects of trisomic gene dosage in total CSA were further understood by examining other cortical parameters. At 6 weeks of age, all control as compared Dp1Tyb mice together had a larger marrow area, cortical area, cortical thickness, periosteal bone surface (Ps.BS), endosteal bone surface (Es.BS), Imax, and Imin. Male as compared to female mice overall exhibited greater cortical area, Imax and Imin (**Table 1 & Fig. 2**). In addition to a reduction in cortical structural parameters, Dp1Tyb mice exhibited lower tissue mineral density (TMD) compared to their wild-type counterparts.

At 16 weeks of age, male control mice had larger total CSA, cortical area, Ps.BS, Es.BS and Imax compared to all other mice, with male mice as a group with higher parameters compared to female mice, and female Dp1Tyb mice having the lowest measurements (**Table 1 & Fig. 2**). Marrow area and Imin are greater in male control than all other mice, and female control are greater than female Dp1Tyb mice for these same parameters. Female mice as a group had reduced cortical thickness compared to male mice. These data suggest that the smaller total CSA in male Dp1Tyb as compared to control mice at 6 and 16 weeks is due to reduced Ps.BS, Es.BS, cortical thickness and marrow area at both ages. In female mice, total CSA appears unchanged and cortical area and thickness is increased from 6 to 16 weeks with decreases in Es.BS and marrow area.

3.5 Mechanical Bone Parameters Exhibit a Sexual Dimorphism in Extrinsic Bone Properties in Dp1Tyb and Control Mice.

The interactive effect and main effect of genotype were significant when all mechanical parameters at 6 weeks were analyzed together by MANOVA, and the sex effect was marginal ($p=0.100$). Interactive, sex, and genotype effects were all significant at 16 weeks when mechanical parameters were analyzed together by MANOVA. At 6 weeks of age in the mechanical properties of extrinsic bone (properties based on bone mass and geometry), the only sex × genotype interaction was for stiffness, with male euploid mice having greater stiffness than all other mice. Control as compared to Dp1Tyb mice at 6 weeks exhibited higher yield force (bone undergoes permanent deformation), ultimate force (measuring general strength of bone), postyield work (energy absorbed after permanent deformation), and total work (total energy absorbed by the bone during bending). Male as compared to female 6-week-old mice also showed a higher ultimate force.

(**Table 2 and Fig. 3**). At 16 weeks of age, the only sex × genotype interaction for extrinsic bone properties was for ultimate force, with control males greater than all other mice and Dp1Tyb males greater than Dp1Tyb females. Control as compared to Dp1Tyb mice at 16 weeks of age had a higher postyield displacement, stiffness, postyield work, and total work; and Dp1Tyb as compared to control mice displayed higher values of displacement to yield and work to yield. At 16 weeks of age, males as compared to females had higher measurements for stiffness, postyield work, and total work (**Table 3 and Fig. 3**).

3.6 Dp1Tyb and Female Mice Appear to have Improved Intrinsic Bone Properties

At 6 weeks of age there were no effects in the intrinsic properties (material properties independent of size and shape) of bone in Dp1Tyb as compared to control or male as compared to female mice. At 16 weeks, control males had a lower modulus (stiffness of material) than all other mice (sex × genotype interaction), and both female and male Dp1Tyb mice had a higher modulus than their control littermates (**Table 3 and Fig 3**). Also at 16 weeks, bone from Dp1Tyb as compared to control mice displayed a higher yield stress (normalized force to size and shape of bone), ultimate stress, and resilience. Control as compared to Dp1Tyb mice had a higher total strain. Female mice had marginally increased yield stress as compared to male mice.

3.7 Histomorphometric Analysis of Cellular Properties show Sex Effects in Dp1Tyb and Control Mice

To understand more about the cellular properties of the femur at 16 weeks when sex and genotypic dimorphisms in intrinsic and extrinsic properties are observed, we analyzed dynamic properties in both cortical (femur midshaft) and trabecular (distal femur) bone. In addition, but not related to mechanical assessment, we analyzed static properties in the trabecular bone of 16-week-old male and female Dp1Tyb and control littermate mice. In cortical bone on the periosteal surface, male as compared to female mice showed increased MS/BS ($p<0.001$, percentage of bone undergoing active formation, and an estimate of osteoblast activity), BFR ($p=0.04$, measure of the total rate of new bone formation on the surface being mineralized) and MAR ($p=0.04$, osteoblast vigor, the rate at which osteoblasts lay down new bone matrix or osteoid) (**Fig. 4A-C**). On the endocortical surface, male control as compared to all other mice had a smaller MS/BS ($p=0.008$)

(sex × genotype interaction). Male control as compared to all female mice had a smaller BFR ($p=0.04$) (sex × genotype interaction) (**Fig. 4D-F**).

In the trabecular bone, there was an increase in female control as compared to male control bone in MS/BS ($p=0.02$) and BFR ($p=0.02$) (sex × genotype interaction) (**Fig. 5A-C**). Bone from female as compared to male mice exhibited a higher trabecular MAR ($p=0.02$) at 16 weeks of age (**Fig. 5C**). Osteoid surface per bone surface (OS/BS) ($p=0.04$) and OS/BS percentage ($p<0.001$) were also greater in trabecular bone of female as compared to male mice. Male Dp1Tyb mice had a lower osteoclast number on the bone surface (Oc#/BS) as compared to all other mice at 16 weeks of age (sex × genotype interaction, $p=0.02$) (**Fig 5D**) as measured by Tartrate-resistant acid phosphatase (TRAP) labeled multinucleated osteoclasts. Additionally, the percentage of bone surface covered by osteoclasts (OcS/BS) was significantly reduced in male as compared to female ($p=0.004$) and control as compared to Dp1Tyb ($p=0.0001$) mice (**Fig 5D**).

When comparing only mice of the same sex, we observed a marginally increased trabecular osteoblast activity and vigor in 16-week-old male Dp1Tyb male as compared to control mice (MS/BS: $p=0.04$, and BFR $p=0.10$, 2 tailed T test). In 16-week-old female mice, there was a suggestive decrease in Dp1Tyb as compared to control mice in trabecular MS/BS and BFR ($p=0.11$ and $p=0.09$, 2 tailed T test). There was reduced trabecular bone osteoclast surface and number in the distal femur of male Dp1Tyb as compared to control littermates at 16 weeks of age ($p<0.001$, 1 tailed T test). In female mice at 16 weeks there was a slight reduction in percent osteoclast number in Dp1Tyb as compared to control animals ($p=0.06$, 2 tailed T test) and no difference in osteoclast surface between Dp1Tyb and control mice in trabecular bone. No difference was found between male Dp1Tyb and control mice in periosteal cortical MS/BS, MAR, or BFR; there was an increase in Dp1Tyb endosteal MS/BS ($p=0.02$, 2 tailed T test) but no differences in endosteal MAR or BFR. There were no significant differences in female periosteal MS/BS, MAR or BFR.

EFFECTS OF OSTEOBLAST SPECIFIC *DYRK1A* REDUCTION IN TS65DN FEMALE MICE

3.7.1 Trabecular Skeletal Deficits in Down syndrome Female Animals

Six week old euploid female mice with two copies of functional *Dyrk1a* (Eu, $Dyrk1a^{+/+}$) had a greater percent bone volume, more Tb.N, and reduced Tb.Sp (**Fig 6)** compared to both trisomic mice with three copies of *Dyrk1a* (Ts65Dn,$Dyrk1a^{+/+/+}$) and trisomic mice with two copies of *Dyrk1a* in the osteoblasts (Ts65Dn, $Dyrk1a^{+/+/-}$). There were no significant differences seen in Tb.Th. Euploid mice with one copy of *Dyrk1a* did not show any significant trabecular deficits compared to either euploid or trisomic mice **(Fig 6)**. These data suggest that significant differences are detected between euploid and trisomic mice and indicating trisomy alters trabecular microarchitecture. Reduced copy number of *Dyrk1a* in osteoblasts did not improve trabecular deficits at this age in female mice (**Fig 6)**. Ts65Dn,$Dyrk1a^{+/+/+}$ and Ts65Dn,$Dyrk1a^{+/+/-}$ had a significantly reduced BMD compared to euploid, suggesting alteration in mineralization in the trabecular compartment (**Fig 9**).

3.7.2 Alteration of Cortical Geometry in Female Ts65Dn Mice

Female Ts65Dn, $Dyrk1a^{+/+/+}$ mice at 6 weeks of age exhibited significant perturbations in cortical parameters as compared to Eu, $Dyrk1a^{+/+}$mice (**Fig 7**). Total CSA was reduced in both trisomic groups as compared to euploid controls (**Fig 7A**). In addition, trisomic mice had a smaller cortical area, marrow area (**Fig 7B&C**) and thickness (**Fig 8A**). Both the periosteal (Ps.BS) and endocortical bone surfaces (Es.BS) were reduced in Ts65Dn, $Dyrk1a^{+/+/+}$ and only Ps.BS was reduced in Ts65Dn, $Dyrk1a^{+/+/-}$ mice compared to Eu,$Dyrk1a^{+/+}$ littermates (**Fig 8B&C**). Therefore, female Ts65Dn, $Dyrk1a^{+/+/+}$ mice exhibited altered cortical geometry compared to controls. Imax and TMD were significantly decreased in both trisomic groups (**Table 4)**.

3.7.3 Extrinsic and Intrinsic Properties in Female Ts65Dn

Female trisomic mice exhibited few significant differences compared to euploid control mice. Ultimate force, postyield and total work were greater in euploid mice compared to both trisomic groups (**Table 5 and Fig 10)**. Total strain was reduced in Ts65Dn,$Dyrk1a^{+/+/+}$ compared

to euploid mice (**Table 5 and Fig 10)**. There were no other differences between genotypes in both extrinsic and intrinsic properties.

3.7.4 Postnatal Death of Ts65Dn,*Dyrk1a*$^{fl/+}$ Male Mice

It had been observed that very few male mice survived with the Ts65Dn,*Dyrk1a*$^{fl/+}$,*Osx*-cre+ genotype, with an expected ratio of 1/8. Upon further analysis it was shown that Ts65Dn,*Dyrk1a*$^{fl/+}$,*Osx*-cre+ male mice were not generated as expected. Because of this phenomenon male mice were excluded from this study. A total of 44 male mice were born and only 2 Ts65Dn,*Dyrk1a*$^{fl/+}$,*Osx*-cre+ mice survived until 6 weeks of age (**Table 6**). We hypothesized that the Ts65Dn,*Dyrk1a*$^{fl/+}$,*Osx*-cre+ genotype was postnatally lethal to male mice. All deceased mice were genotyped to validate this hypothesis. There was a total of 44 mice that died between what ages postnatal day zero (P0) and P42, with 28 males and 15 females that perished. In addition, 30 mice out of all 44 who expired postnally, did not possess *Osx*-cre recombinase. Only 2 male mice out of all 44 mice had the Ts65Dn,*Dyrk1a*$^{fl/+}$,*Osx*-cre+ genotype. The most common age at death was one day after birth, with 24 out of 44 of the dead animals. Ts65Dn,*Dyrk1a*$^{fl/+}$,*Osx*-cre+ does not appear to contribute to postnatal death seen in male mice. It still remains unclear what is causing the male mice to die. Further investigations into possible factors related to the absence of Ts65Dn,*Dyrk1a*$^{fl/+}$,*Osx*-cre+ mice amongst the genotypes will be explored, including examining embryos to determine if male mice die before birth.

3.7.5 Confirmation of Cre-mediated Deletion of *Dyrk1a* in Osteoblasts.

All mice were genotyped before death and mice that were positive for *Osx*-cre were analyzed to determine if cre-mediated deletion was successful. *Dyrk1a* is floxed between exons 5 and 6, after cre-mediated deletion exon 4 is then joined with exon 7. Primers were generated to identify the Floxed deletion allele spanning the novel sequence between the rejoined exon 4 and exon 7. The presence of a 214bp band, confirmed deletion of exons 5 and 6 of *Dyrk1a*. Extraction of osteocyte DNA from the tibia of *Osx*-cre female mice were analyzed to detect the confirmation of cre-mediated deletion, presence of trisomy and *Dyrk1a*$^{fl/+}$. Preliminary data of 10 *Osx*-cre+ female mice that were genotyped to confirm, via PCR, the presence of a *Dyrk1a*$^{fl/+}$ allele, trisomy and *Osx*-cre recombinase. 8 out of 10 mice that were positive for *Dyrk1a*$^{fl/+}$ and *Osx*-cre+

generated a Floxdel allele, confirming *Dyrk1a* was reduced in osteoblasts and osteocytes. Also, there were no changes from their original genotype. The 2 remaining mice that were negative for *Dyrk1a*$^{fl/+}$ and *Osx*-cre+, and produced Floxdel product, suggesting a possible change in genotype, specifically they were mis-genotyped.

CHAPTER 4. DISCUSSION

4.1 Interaction of Sexual Dimorphism and Genetic Dosage Imbalance in Dp1Tyb Mouse Model

The novel examination of male and female mice in the Dp1Tyb mouse model of DS during typical times of bone accrual and skeletal maturity revealed the effect of both the sex of the mouse and the presence/absence of three copies of dosage sensitive genes on skeletal phenotypes associated with DS. Here we report the first evidence of sexual dimorphism in skeletal deficits of DS model mice that parallels differences between skeletal deficits in humans with DS of different sexes. The non-invasive quantification of bone deficits in humans with DS gives insight into some parameters, including BMD, but does not provide information on the geometry or composition of bone. BMD is a metric used to calculate risk factor for fracture, however, many studies do not include geometry, structural and strength indices that also affect fracture incidence (Fowler et al., 2012; Gonzalez-Aguero, Vicente-Rodriguez, Gomez-Cabello, & Casajus, 2013). Until recently, studies of bone in individuals with DS have often been done using small sample sizes that may have not been able to detect important changes in bone between males and females with DS during various developmental time points. Using mouse models of DS allows for the quantification of structural, mechanical and cellular properties during different times of bone development. The data obtained show clear age, sexual, and genotypic differences in several measures that recapitulate many phenotypes observed in individuals with DS, especially at formative developmental stages.

At 6 weeks of age, trabecular parameters including BV/TV, Tb.Th, Tb.N and Tb.Sp are adversely affected in both Dp1Tyb and wild-type littermate female mice and are at similar levels as Dp1Tyb male mice. Although females have reduced trabecular measures compared to male wild-type mice at 6 weeks of age, trisomy does not further reduce those measures. These data suggest a protective effect of female sex against trisomic defects during longitudinal bone growth. As mice reach the age of skeletal maturity at 16 weeks, BV/TV of female mice has not increased; furthermore, Tb.N has decreased and Tb.Th and Tb.Sp have increased in both Dp1Tyb and wild-type mice. In female mice, the reduction in Tb.N and increase in Tb.Sp may have negatively influenced connectivity to the point that even with increased Tb.Th at 16 weeks, skeletal measurements are still adversely affected.

Male Dp1Tyb present with a reduction of percent bone volume at 6 weeks and is persistent until 16 weeks age suggesting that the process of bone formation is negatively activate during adolescence (active growth) and sexual maturity. Male control and Dp1Tyb mice develop trabecular bone between 6 and 16 weeks consistent with a normal growth pattern, however Dp1Tyb mice exhibit structural deficits compared to control mice.

Female mice gain Tb.Th and Tb.Sp, while theylose Tb.N and BV/TV between 6 and 16 weeks. Thus, indicating reduced bone formation or increased resorption across ages. Trabecular deficits in female mice appear to be independent of genotype at both 6 and 16 weeks. Taken together, these results show that trisomy has little effect on the trabecular microarchitecture of female mice but could contribute to a decrease in bone formation or an increase in resorption of trabeculae.

At 6 and 16 weeks, Dp1Tyb male and female mice generally have deficits in cortical geometry as compared to their wild-type counterparts. The total CSA increased in male but not female mice from 6 to 16 weeks of age. Measures of cortical bone in male and female Dp1Tyb mice are similar at 6 weeks. Female mice as a group do not have increases of total CSA across ages, but exhibit decreases in marrow area and an increase in cortical area. Dynamic histomorphometry of the femoral midshaft suggests this increase is largely due to increased activity of osteoblasts on the endocortical surface in female mice suggesting endocortical contraction. Changes in cortical geometry for control and Dp1Tyb mice in the cortical bone follows a normal pattern of skeletal growth, with three copies of genes enhancing deficits in female mice.

4.1.1 *Dyrk1a* Genetic Dosage in Osteoblast in Female Ts65Dn,*Dyrk1a* Mice in Trabecular and Cortical Microarchitecture

At 6 weeks of age, trisomic female mice have detrimental trabecular deficits compared to euploid mice. There is a distinct phenotype between genotypes that is absent in Dp1Tyb female animals. Both trisomic animals, Ts65Dn, *Dyrk1a*$^{+/+/+}$ and Ts65Dn, *Dyrk1a*$^{+/+/-}$ have attenuated BV/TV and Tb.N with increased Tb.Sp. Therefore, female trisomic mice either exhibited an impairment in bone formation or increased resorption of trabeculae. Decreased copy number of *Dyrk1a* in osteoblasts in no way altered or improved trabecular deficits observed in trisomic animals and did not adversely affect euploid mice with only one functional copy of *Dyrk1a*.

Female trisomic mice at 6 weeks of age, in Ts65Dn, *Dyrk1a*$^{+/+/+}$ and Ts65Dn, *Dyrk1a*$^{+/+/-}$ exhibited decreased Total CSA, and cortical area emphasizing reduce bone size and confirmed by a reduction in cortical thickness and TMD. These alterations suggest possible deficits either in diminished bone accrual or increased resorption via cortical thinning. Furthermore, female trisomic and knockdown animals have a smaller Ps.BS, and only trisomic animals exhibit a reduction in Es.BS highlighting differences in bone maintenance between groups. Ts65Dn, *Dyrk1a*$^{+/+/-}$ animals did not have a reduced marrow area compared to euploid controls, possibly indicating alterations in bone accrual or maintenance of the medullary cavity compared to Ts65Dn,*Dyrk1a*$^{+/+/+}$ animals.

This is a novel trisomic phenotype seen in Ts65Dn female trisomic mice and is contrary to what is observed in Dp1Tyb female animals. Differences in trisomic genetic content and background might contribute to specific phenotypes associated to female Dp1Tyb and Ts65Dn**,** *Dyrk1a*$^{+/+/-}$ and Ts65Dn, *Dyrk1a*$^{+/+/+}$ skeletal deficits in femoral architecture. Observed differences in skeletal phenotypes between Dp1Tyb and Ts65Dn can contribute to ongoing debate concerning the effectiveness of specific mouse models to recapitulate human phenotypes associated with DS. Identification of molecular or cellular mechanisms responsible for the etiology of disruption of bone homeostasis remains unclear, and the use of appropriate mouse models is essential to their discovery.

4.2 Trabecular and Cortical Phenotype Comparison of Dp1Tyb, Female Ts65Dn and Other DS Model Mice

Bone deficits associated with DS were first identified in Ts65Dn male mice (Blazek et al., 2011). A comparison between these and previously published results reveals similar direction and magnitude in trabecular, cortical and mechanical deficits in mice that are at dosage imbalance for genes homologous to Hsa21 (Blazek, Abeysekera, et al., 2015; Blazek et al., 2011). Previous studies of 6, 12, 16 week, and 24 month old male mice found no significant differences in trabecular thickness (Tb.Th) between Ts65Dn and euploid mice, though these values were near a $p<0.05$ significance level (Blazek et al., 2011; Fowler et al., 2012). Tb.Th was significantly different between Ts65Dn and control mice at 6 weeks of age and were corrected in Ts65Dn,*Dyrk1a*+/- mice in a subsequent study (Blazek, Abeysekera, et al., 2015). The differences in Tb.Th between Dp1Tyb and wild-type mice seem to confirm the dissimilarities in the later study.

The data presented confirm that the Dp1Tyb DS mouse model is an effective model for skeletal deficits in male and female DS model mice.

Ts65Dn, *Dyrk1a*$^{+/+/-}$ mice had a spatiotemporal reduction of *Dyrk1a* copy number in osteoblast cells expressing *Osx*. Ts65Dn, *Dyrk1a*$^{+/+/-}$ and Ts65Dn, *Dyrk1a*$^{+/+/+}$ mice each demonstrated skeletal deficiencies in T.Sp, Tb.N, and BV/TV; similar to observed phenotypes between male Ts65Dn mice and Dp1Tyb compared to euploid controls (Blazek, Abeysekera, et al., 2015). In contrast, Ts65Dn, *Dyrk1a*$^{+/+/-}$(affecting only mature osteoblasts) did not display any correction of trabecular or cortical defects as seen in male Ts65Dn, *Dyrk1a*$^{+/-}$(global deletion of *Dyrk1a*) from Blazek et al, 2015a (Blazek, Abeysekera, et al., 2015). Additionally, Ts65Dn, *Dyrk1a*$^{+/+/-}$ and Ts65Dn, *Dyrk1a*$^{+/+/+}$ showed more significant differences between euploid controls, which was not observed between female Dp1Tyb and control animals both at 6 weeks of age. Differences between Dp1Tyb and Ts65Dn skeletal anomalies could arise from genetic background and gene dosage, which is discussed later in this manuscript.

Male and female Ts1Rhr mice, containing 33 triplicated genes, at 3 and 16 weeks have been examined for bone deficits associated with DS (Olson & Mohan, 2011). At 3 weeks (a developmental age prior to where we identified differences in BV/TV at 6 weeks in Dp1Tyb and control littermate female mice), BMD was not statistically different between male or female Ts1Rhr or control mice. It may be that BMD is not significant between Ts1Rhr and control male mice at this pre-pubertal age. At 16 weeks, in Ts1Rhr and littermate control mice, areal BMD was not significantly different in the femur, but was decreased in the tibia and increased in the spine. Our analyses of Dp1Tyb and littermate mice found significantly different trabecular BMD between both male and female mice at 16 weeks of age. Further studies, including microCT, were not performed on the bones of Ts1Rhr and control littermate mice, and given the analyses included herein, we hypothesize that other structural and mechanical bone abnormalities exist between Ts1Rhr and control mice. Conversely, the reduction in genes at dosage imbalance in Ts1Rhr as compared to Dp1Tyb mice could dilute any potential effect from triplicated genes.

Differences between skeletal abnormalities could also be due to genetic background, number and which genes are at dosage imbalance, and origin of the change in genetic dosage. Differences in skeletal phenotypes could be due to differences in triplicated gene content or genetic background of Ts65Dn (104 genes, ~50% B6 and ~50% C3H) and Dp1Tyb (148 genes, 100% B6) and Ts1Rhr (33 genes, 100% B6) mice. Differences in trisomy may also contribute to skeletal differences

between mouse models. Ts65Dn has a freely segregating extra chromosome with the telomeric end of Mmu16 attached to the centromeric end of Mmu17. This includes ~35 protein-coding genes at dosage imbalance from Mmu17 that are not homologous to Hsa21 (Duchon et al., 2011; Gupta et al., 2016; Reinholdt et al., 2011). Both Dp1Tyb and Ts1Rhr mice have a duplication of parts of the distal end of Mmu16 and do not have a freely segregating trisomic chromosome. All of these factors may lead to differences between the DS mouse models that have been used to detect skeletal abnormalities associated with DS. We note that as the gene content of Dp1Tyb mice is known, it may now be possible to look for the causal genes for bone defects, i.e. those sequences on Hsa21 that have an effect when present in three copies.

4.3 Similarities Between Humans with DS and Mouse Models with DS

It is hypothesized that the osteoporotic phenotype found in individuals with DS is highly influenced by limited bone mineral accretion and reduced peak bone mass attainment during adolescence (Costa et al., 2018; Tang et al., 2019). In humans the age of total body peak bone mass has been estimated to be about 18.8 years in females and 20.5 years in males (Baxter-Jones, Faulkner, Forwood, Mirwald, & Bailey, 2011). Individuals with DS attain peak bone mass earlier and at lower levels than normal individuals (Costa et al., 2018). Women with DS (as well as normal women) have bone mineral accrual later than men, but experience rapid bone loss after the age of 40 (Tang et al., 2019). Men with DS have a gradual loss of bone after early adulthood, similar to men without DS, but the rate of loss is increased in men with DS (Carfi et al., 2017; Tang et al., 2019).

Information from the analyses described herein concentrated on skeletal properties during bone accrual (6 weeks) until the estimated age of skeletal maturity in mice (16 weeks) (Jilka, 2013). There are few studies that have examined DS skeletal deficits in humans during adolescence and the time of peak bone accrual, and the results from Dp1Tyb male and female mice may help explain previous reports. The lower BMD seen in adolescent males and females with DS analyzed together as compared to normal individuals (Kao et al., 1992; Matute-Llorente et al., 2013) compares to the genotype effect causing low BV/TV (and BMD) in 6-week Dp1Tyb mice. A study of adolescents with DS that found no differences in BMD between males and females (Matute-Llorente et al., 2017) correlates to the similar BV/TV levels in 6 week old male and female Dp1Tyb mice. At an age corresponding to skeletal maturity in individuals with DS, both males and females had a lower

BMD (Angelopoulou et al., 1999), with DS females having a lower BMD than DS males in their limbs (Baptista et al., 2005); both male and female Dp1Tyb mice had significantly affected bone structure at 16 weeks, and trabecular and cortical values were significantly lower in females than males at 16 weeks. The data presented herein also demonstrate that male Dp1Tyb mice exhibit osteopenic phenotypes earlier than their control counterparts, similar to what has been observed in individuals with DS (Carfi et al., 2017; McKelvey et al., 2013) and that osteoporotic phenotypes affect males as well as females in early adult stages (Tang et al., 2019).

4.4 Mechanical Properties of Dp1Tyb Mice

Bone is hierarchical and alterations in bone composition, architecture, and cellular activity can increase or decrease bone strength. Our results suggest changes in cortical geometry possibly contributed to differences observed in mechanical properties of Dp1Tyb and WT mice. At 6 weeks of age, most of the significant differences between Dp1Tyb and control mice were found in whole bone properties. In general, control and male mice at 6 and 16 weeks had stronger bones or greater resistance to bending and catastrophic failure compared to their Dp1Tyb counterparts. Genetic dosage imbalance could be sufficient to cause alterations in the developing skeleton of male mice resulting in reduced strength of femur.

At 16 weeks enhanced effects on bone tissue, independent of bone size and shape, were observed. Female as compared to male mice displayed an increase in yield stress but had marginally lower toughness. These changes in material properties of bone in Dp1Tyb mice may indicate changes in mineralization of the femur and possibly result in bones that are more prone to fracture. Dp1Tyb mice showed an increase in yield properties in both the load-displacement and stress-strain curves. Increases in yield properties are related to bone mineral content and post-yield properties associated with collagen (Garnero, 2015). Dp1Tyb mice had lower toughness, post yield work and total work, suggesting they absorbed less energy prior to fracture and possibly fracture sooner than control animals.

Taken together, these data indicate that there was a strong genotypic effect at 6 weeks in extrinsic bone properties but at 16 weeks, sex and especially genotype had non-interactive effects on overall bone properties. At 16 weeks of age, additional gene dosage and female sex were detrimental to whole bone properties. Additional, Dp1Tyb and female mice at 16 weeks seem to have alterations in material bone properties as compared to control and male mice. This is observed

especially in the elastic region before the bone becomes permanently deformed, correlating to significant changes in mineralization in females.

4.4.1 Mechanical Properties in Female Ts65Dn, *Dyrk1a*$^{fl/+}$*Osx*-Cre Animals

Unexpectedly, there were not many differences in whole bone properties or material properties between female euploid and trisomic mice based on three-point bending analysis. Ultimate force was significantly decreased in female trisomic and Ts65Dn,*Dyrk1a*$^{+/+/-}$ mice, indicating there was reduced bone strength compared to euploid animals. Reduction in total work was shown also in both trisomic groups compared to euploid mice. Therefore, trisomic animals absorb less energy meaning a reduced ability to deal with damage and overall strength. Lastly, total strain was reduced in trisomic animals highlighting reduced ductility. In contrast, Ts65Dn,*Dyrk1a*$^{+/+/+}$ and Ts65Dn,*Dyrk1a*$^{+/+/-}$ mice had reduced TMD in cortical bone. There were no other differences between genotypes in both extrinsic and intrinsic properties. These findings suggest there might be alterations in the material properties in female trisomic mice that contribute to resistance to deformation.

4.5 Cellular Deficits in Mouse Models of DS

Quantification of cellular composition in trabecular and cortical bone in 6-week-old male Ts65Dn as compared to control mice showed reduced osteoblast number and/or activity coupled with increased osteoclast activity caused the DS like skeletal deficits at that age (Blazek, Abeysekera, et al., 2015; Blazek et al., 2011). A low bone turnover hypothesis was proposed for the deficits skeletal deficits seen in 12-week-old male Ts65Dn mice because of decreased osteoclast and osteoblast activity found on proximal tibia and femur as compared to euploid mice at this age (Fowler et al., 2012). In 16-week-old male mice, we observed increased osteoblast activity and reduced osteoclast number and activity in the trabecular compartment of Dp1Tyb as compared to control mice. In female mice of the same age, there was a decrease in Dp1Tyb osteoblast activity. These results indicate that osteoblast and osteoclast activity was different in 16-week-old male Dp1Tyb mice than previously reported osteoblast and osteoclast activity in Ts65Dn mice at 6 and 12 weeks (Blazek, Abeysekera, et al., 2015; Fowler et al., 2012). Only a slight increase in osteoblast activity on the periosteal surface of male Dp1Tyb cortical bone was

observed. These data support the notion that male mice are more active in forming bone on the periosteal surface while female and trisomic mice are more active in forming bone on the endocortical surface at 16 weeks of age. Therefore, sex, gene dosage, bone location and age are all important in the cellular components Dp1Tyb as compared to control mice. Furthermore, the cellular mechanisms leading to bone deficits associated with DS may be distinct at different points in development.

These data demonstrate fundamental differences in skeletal development between Dp1Tyb and wild-type mice. For the first time, they also indicate clear sexual dimorphisms in the development of DS mouse model bone and illustrate time-dependent nature of developmental differences in the DS-associated skeletal deficits. Similarities between the abnormalities in humans with DS and Dp1Tyb mice suggest that skeletal defects result from conserved mechanisms. Sexual dimorphisms, gene dosage, age and bone compartments are all influential in causing alterations in developmental properties that lead to the unique skeletal differences caused by trisomy. These results will help to better understand how trisomy affects individuals with DS and determine which measures may prevent adverse skeletal phenotypes. Additional research is needed to determine when sex-specific skeletal abnormalities develop, how interactions between trisomy and sex influence specific skeletal alterations, and the influence of sex and trisomy on the cellular mechanisms related to these changes in bone development.

4.5.1 Cre-mediated Deletion of One Functional Copy Number of *Dyrk1a*

PCR was performed to detect confirmation of their prior genotype for *Dyrk1a*$^{fl/+}$, trisomy and *Osx*-cre. Each mouse was compared to original genotype to detect any changes and the Floxdel allele. Female *Osx*-cre+ mice that contain at least one floxed allele have exhibited a Floxdel positive band. This suggests that *Dyrk1a* copy number has been reduced under the *Osx* promoter. However, based on PCR analysis of DNA obtained from female tibiae, has shown the *Dyrk1a*$^{fl/+}$ allele is present in majority of animals except two out of a total of 10. It is possible that other cells are present in the sample besides osteoblasts and osteocytes, or that there was an incomplete deletion of the floxed *Dyrk1a* allele. Further analysis of remaining female *Osx*-cre+ animals is needed to determine efficiency of Cre-mediated deletion of *Dyrk1a* in osteoblasts and osteocytes.

4.6 Future Direction

Dp1Tyb analysis of bone deficits provided the establishment of differences in skeletal deficits between male and female mice. We observed little to no significant differences between control female and Dp1Tyb female trabecular architecture and cortical geometry at 6 weeks of age. This might suggest a protective effect of female compared to males in the onset of skeletal abnormalities. Additional investigations into different ages of DS mice could elucidate possible developmental timepoints related to the onset of bone deficits. These protective effects could be the result of differential expression of trisomic genes, bone turnover markers or hormonal levels. Measurements of each of these possible culprits could identify possible differences between males and females and the contribution of Ts21 in the onset of skeletal anomalies.

Dyrk1a has been shown to improve skeletal deficits in several studies, emphasizing its role in skeletal development. Previous studies reduced copy number of *Dyrk1a* globally, whereas in this study genetic dosage was reduced only in OSX expressing osteoblasts and mature osteocytes. There was little to no benefit seen in female Ts65Dn, $Dyrk1a^{+/+/-}$ animals in both microarchitecture and biomechanical properties in female animals. Investigating cell types other than osteoblasts that might contribute to skeletal deficits in Ts65Dn, $Dyrk1a^{+/+/-}$ female mice could reveal novel mechanisms related to bone accrual, mineralization and homeostasis. Observing skeletal deficits in male Ts65Dn, $Dyrk1a^{+/+/-}$ and Ts65Dn, $Dyrk1a^{+/+/+}$ mice could identify a possible sexual dimorphism in Ts65Dn mice and uncover differences in skeletal development and maintenance between genotypes.

DYRK1A has been shown to play a complex role in osteoclast number and increased expression of DYRK1A could affect osteoclastogenesis. Reducing DYRK1A in osteoclasts could rescue the perturbations in the regulation of osteoclastogenesis, maturation or survival. It has been shown that DYRK1A has interactions with other osteoclastic factors including NFATc, Akt, and Erk. NFATc is a pro-osteoclastic factor that is negatively regulated by DYRK1A which could result in decreased osteoclastogenesis (Arron et al., 2006; Lee et al., 2009). Akt and Erk have been shown to play a role in osteoclast differentiation and resorptive activity (Abekhoukh et al., 2013; He et al., 2011; Moon et al., 2012). DYRK1A overexpression may negatively regulate skeletal development and homeostasis via osteoclastic pathways as opposed through alterations in osteoblast activity and differentiation.

Global reduction of *Dyrk1a*rescued skeletal deficits seen in Ts65Dn animals as seen in our previous study (Blazek, Abeysekera, et al., 2015). This correction of the skeletal phenotype was not seen in trisomic Ts65Dn mice with reduced copy of *Dyrk1a* in osteoblasts under the *Osx* promoter. Therefore, abnormal skeletal phenotypes associated with DYRK1A overexpression may not be specific to osteoblasts and does not account for origin of all skeletal anomalies seen in DS. It is hypothesized that global reduction of *Dyrk1a* affected multiple cell types during all stages of development. Regulation skeletal development and maintenance are controlled by various cytokines, growth factors cell-cell communication and interactions with extracellular matrices. Moreover, reduction of *Dyrk1a*in other cell types, besides just osteoblasts, could be responsible for the amelioration of skeletal abnormalities. Therefore, it could be suggested that *Dyrk1a* alters the balance between bone resorption and formation leading to osteopenic phenotypes seen in Ts65Dn animals. Identification of other molecular targets associated with *Dyrk1a*expression could highlight novel developmental pathways associated with skeletal growth, development and homeostasis. Future investigations into the cellular or molecular mechanisms that contribute the bone phenotype are needed to elucidate specific contributions to the origin of skeletal abnormalities.

APPENDIX A. DP1TYB INTERACTION OF SEXUAL DIMORPHISM AND DOSAGE SENSITIVE GENES IN SKELETAL DEFICITS ASSOCIATED WITH DOWN SYNDROME

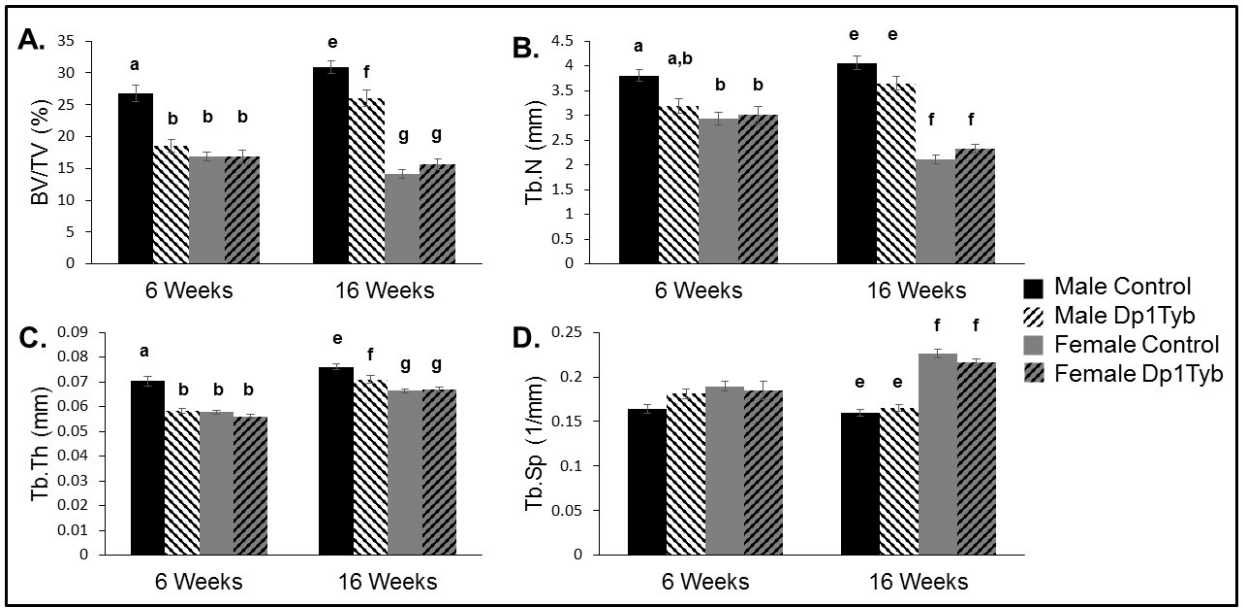

Figure 1 - Trabecular measures on Dp1Tyb and littermate control femurs at 6 and 16 weeks (mean +/- SEM). MANOVAs on the combined four trabecular parameters, performed separately for the 6- and 16-week data, respectively, indicated significant sex × genotype interactive effects (p=0.001, p=0.001), along with significant main effects of sex (p<0.001, p<0.001) and genotype (p<0.001, p=0.003). The individual parameters are depicted in the four panels: (A) Percent bone volume (BV/TV); 6 weeks: sex × genotype interaction: p=0.044, [ηp2=0.103]; genotypic effect: p=0.001, [ηp2=0.275], and sex effect: p<0.001, [ηp2=0.426]; 16 weeks: sex × genotype interaction: p=0.001, [ηp2=0.164]; genotypic effect: p=0.069, [ηp2=0.056], and sex effect: p<0.001, ηp2=0.785. (B) Trabecular number (Tb.N): 6 weeks: sex × genotype interaction: p<.001, [ηp2=0.268]; genotypic effect: p=0.097, [ηp2=.071], and sex effect: p=0.003, [ηp2=0.209]; 16 weeks: sex × genotype interaction: p=0.009, [ηp2=.112]; genotypic effect: p=0.345, [ηp2=0.015], and sex effect: p<0.001, ηp2=0.779. (C) Trabecular thickness (Tb.Th): 6 weeks: sex × genotype interaction: p<0.001, [ηp2=0.283]; genotypic effect: p<0.001, [ηp2=0.413], and sex effect: p<0.001, [ηp2=0.446]; 16 weeks: sex × genotype interaction: p=0.015, [ηp2=0.097]; genotypic effect: p=0.021, [ηp2=0.089], and sex effect: p<0.001, [ηp2=0.420]. (D) Trabecular separation (Tb.Sp): 6 weeks: sex × genotype interaction: p=0.174, [ηp2=0.048]; genotypic effect: p=0.431, [ηp2=0.016], and sex effect: p=0.063, [ηp2=0.088]; 16 weeks: sex × genotype interaction: p=0.098, [ηp2=0.046]; genotypic effect: p=0.669, [ηp2=0.003], and sex effect: p<0.001, [ηp2=0.736]. Male control (n=10 6 wk; n=13 16 wk); Male Dp1Tyb; n=10 6 wk; n=11 16 wk); Female control (n=12 6 wk; n=22 16 wk); Female Dp1Tyb (n=10 6 wk; n=16 16 wk). Significant differences and interactions for individual parameters are as determined by ANOVA and the p value is followed by partial eta squared [ηp2] as a measure of effect size. Similarities and differences between individual groups are determined from Tukey's multiple comparisons post hoc tests; values with the same superscript letter are not significantly different. Letters a,b,c,d are used for comparisons of 6 week old animals; letters e,f,g,h are used for comparisons of 16 week old animals.

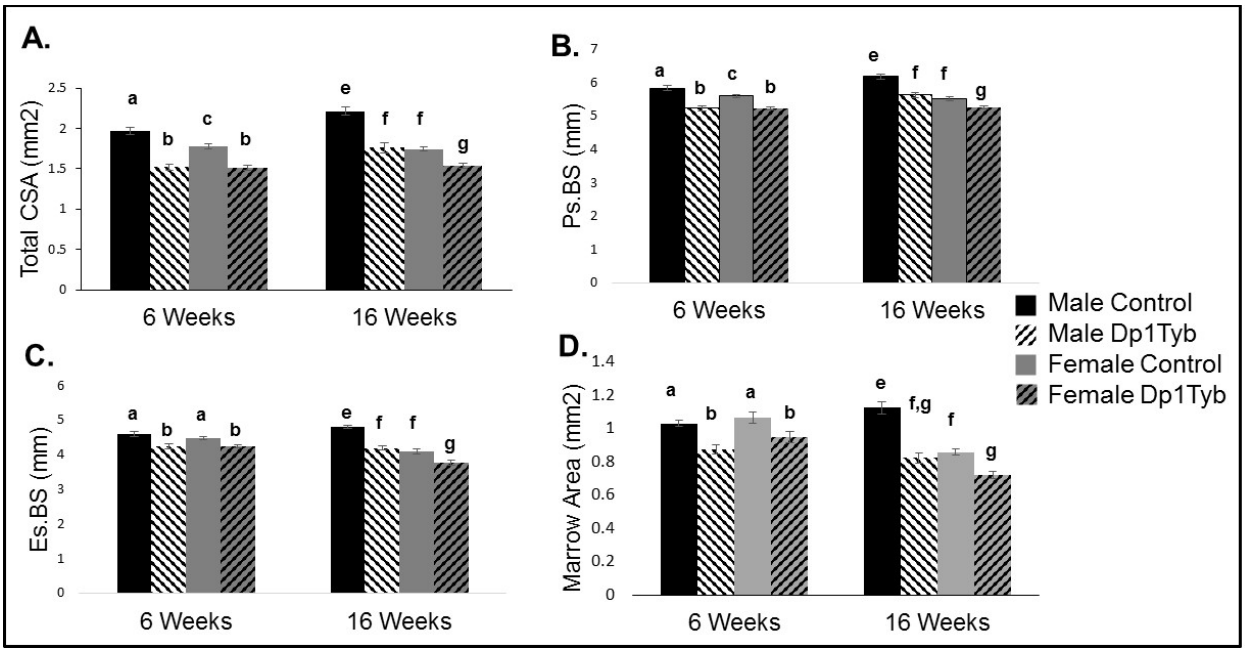

Figure 2 - Cortical measures on Dp1Tyb and control femurs at 6 and 16 weeks (mean +/- SEM). MANOVAs on the combined 16 cortical parameters, performed separately for the 6- and 16-week cortical data, respectively, indicated significant main effects of sex ($p=0.003$, $p<0.01$) and genotype ($p<0.001$, $p<0.001$). The interaction between sex and genotype was significant at 16 weeks p= $p<0.001$) but not 6 weeks ($p=.236$). Four of the 16 individual parameters showing significant sex × genotype interactions at 16 weeks are depicted in the four panels: (A) Cortical total cross-sectional area (CSA): 6 weeks: sex × genotype interaction: $p=0.024$, [$\eta p2=0.127$]; genotypic effect: $p<0.001$, [$\eta p2=0.689$], and sex effect: $p=0.014$, [$\eta p2=0.149$]; 16 weeks: sex × genotype interaction: $p=0.001$, [$\eta p2=0.177$]; genotypic effect: $p<0.001$, [$\eta p2=0.613$], and sex effect: $p<0.001$, [$\eta p2=0.574$]. (B) Periosteal bone surface (Ps.BS): 6 weeks: sex × genotype interaction: $p=0.070$, [$\eta p2=0.084$]; genotypic effect: $p<0.001$, [$\eta p2=0.619$], and sex effect: $p=0.060$, [$\eta p2=0.090$]; 16 weeks: sex × genotype interaction: $p=0.007$, [$\eta p2=.118$]; genotypic effect: $p<0.001$, [$\eta p2=0.590$], and sex effect: $p<0.001$, [$\eta p2=0.624$]. (C) Endocortical bone surface (Es.BS): 6 weeks: sex × genotype interaction: $p=0.343$, [$\eta p2=0.024$]; genotypic effect: $p<0.001$, [$\eta p2=0.396$], and sex effect: $p=0.319$, [$\eta p2=0.026$]; 16 weeks: sex × genotype interaction: $p=0.013$, [$\eta p2=0.101$]; genotypic effect: $p<0.001$, [$\eta p2=0.590$], and sex effect: $p<0.001$, [$\eta p2=0.635$]. (D) Marrow area: 6 weeks: sex × genotype interaction: $p=0.157$, [$\eta p2=0.052$]; genotypic effect: $p<0.001$, [$\eta p2=0.430$], and sex effect: $p=0.238$, [$\eta p2=0.036$]; 16 weeks: sex × genotype interaction: $p=0.002$, [$\eta p2=0.157$]; genotypic effect: $p<0.001$, [$\eta p2=0.607$], and sex effect: $p<0.001$, [$\eta p2=0.467$] in Dp1Tyb and control male and female mice at 6 and 16 weeks. Significant differences and interactions for individual parameters are as determined by ANOVA and the p value is followed by partial eta squared [$\eta p2$] as a measure of effect size. Similarities and differences between individual groups are determined from Tukey's multiple comparisons post hoc tests; values with the same superscript letter are not significantly different. Letters a,b,c,d are used for comparisons of 6 week old animals; letters e,f,g,h are used for comparisons of 16 week old animals.

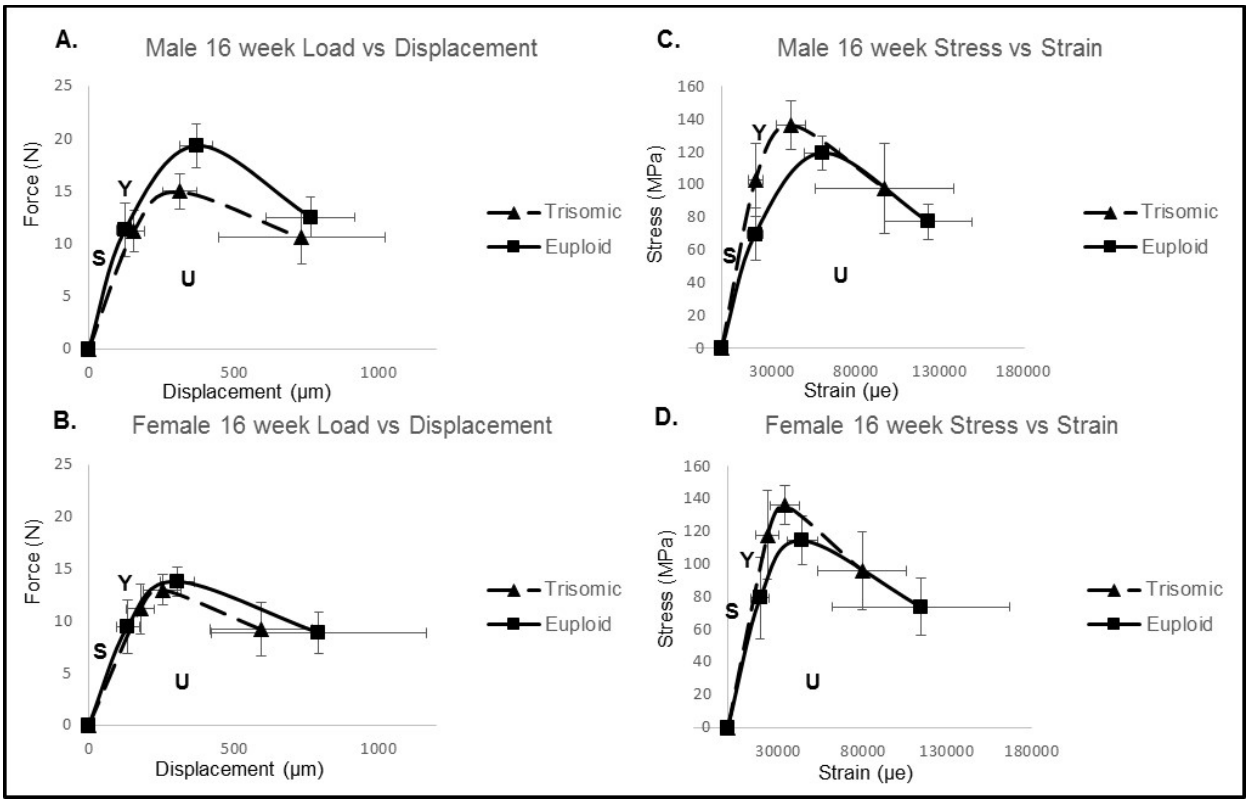

Figure 3 - Schematic representation of mechanical testing curves (data represented by mean ± SEM). A and B) Representations of force-displacement curves at the structural level. C and D) Representations of stress-strain curves at the tissue level. S, is related to the stiffness or modulus of the femur. Y, the yield point represents elastic behavior, indicating the bone's resistance to permanent deformation, past this point, U is the plastic region or permanent deformation where the bone has sustained permanent damage.

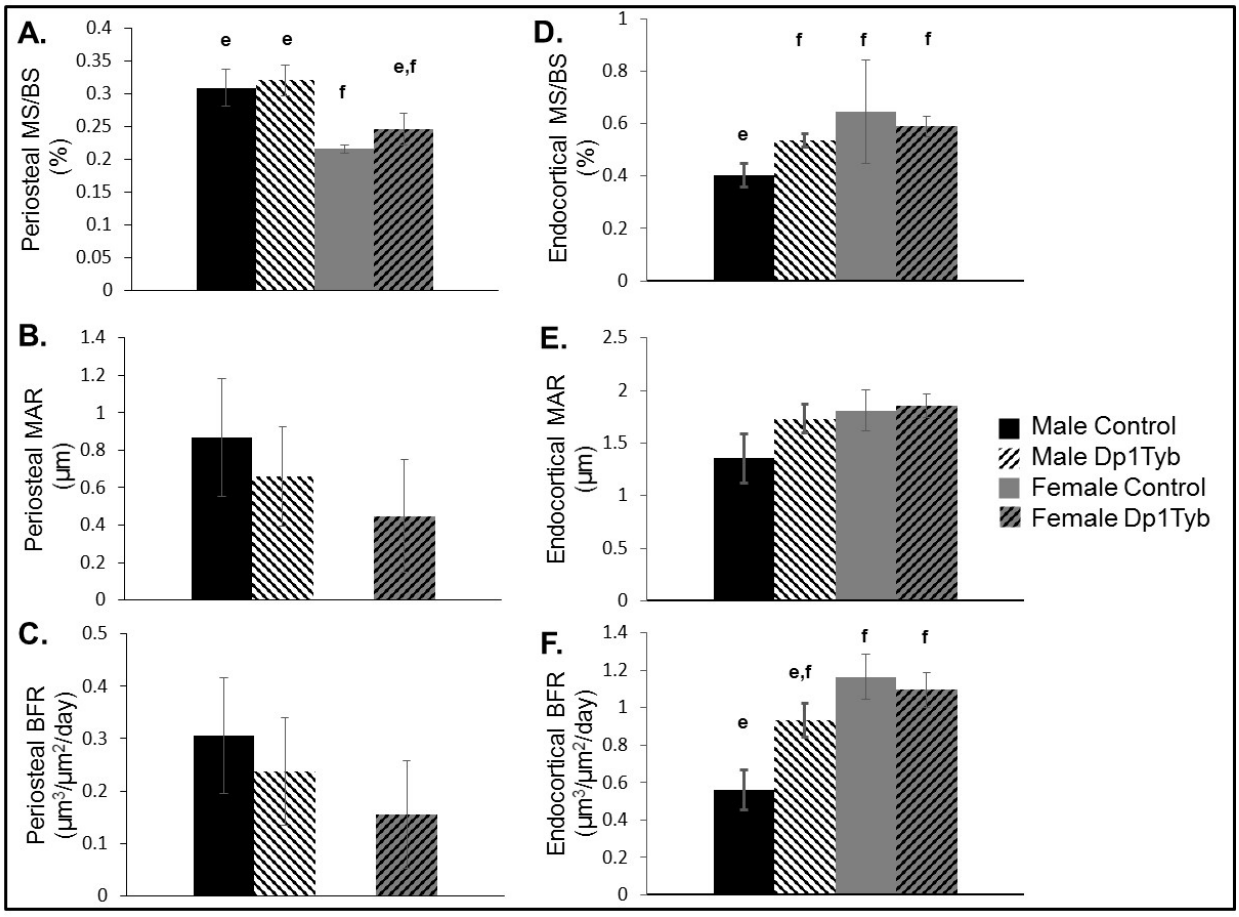

Figure 4 - Dynamic bone labeling measures of the cortical region of Dp1Tyb and control femurs at 16 weeks of age (data represented by mean ± SEM). (A) Periosteal mineralizing surface/bone surface (MS/BS), (B) Periosteal mineral apposition rate (MAR), (C) Periosteal bone formation rate (BFR), (D) Endocortical MS/BS, (E) Endocortical MAR, (F) Endocortical BFR. In (B) and (C), there were no measurable effects in female control MAR and BFR (9 samples in each group). Similarities and differences between individual groups are determined from Tukey's multiple comparisons post hoc tests; values with the same superscript letter are not significantly different. Letters a,b,c,d are used for comparisons of 6 week old animals; letters e,f,g,h are used for comparisons of 16 week old animals.

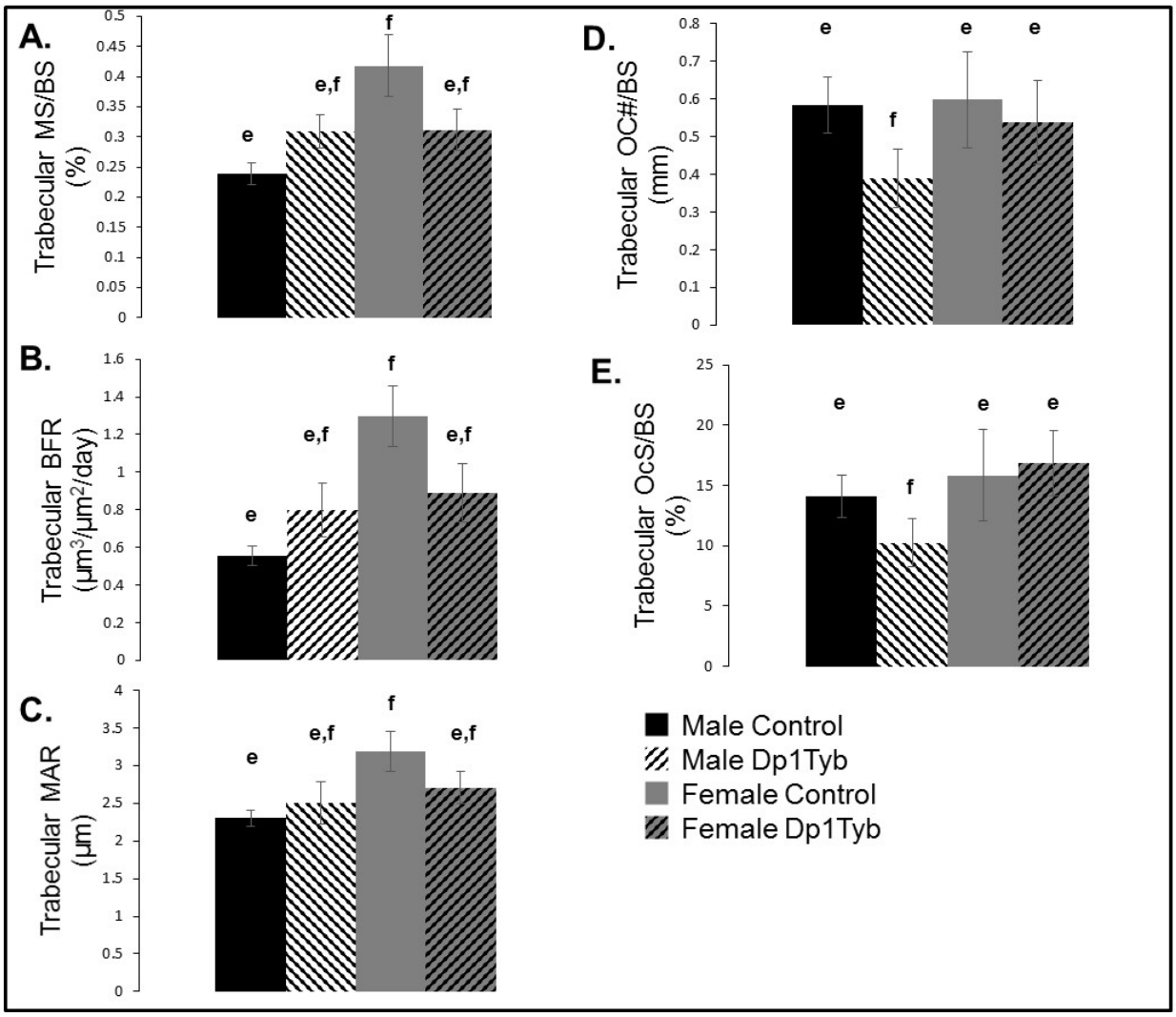

Figure 5- Dynamic bone labeling quantification of the trabecular region of Dp1Tyb and control femurs at 16 weeks of age (data represented by mean ± SEM). (A) Trabecular mineralizing surface/bone surface (MS/BS), (B) Trabecular mineral apposition rate (BFR), (C) Trabecular bone formation rate (MAR), (D) Osteoclast number/bone surface (OC#/BS), (E) Osteoclast surface/bone surface. Similarities and differences between individual groups are determined from Tukey's multiple comparisons post hoc tests; values with the same superscript letter are not significantly different. Letters a,b,c,d are used for comparisons of 6 week old animals; letters e,f,g,h are used for comparisons of 16 week old animals.

Table 1: Cortical Architecture and Geometry of Dp1Tyb and Control Male and Female Mice at 6 and 16 Weeks

	Male Control 6 Weeks	Male Dp1Tyb 6 Weeks	Female Control 6 Weeks	Female Dp1Tyb 6 Weeks	Between subjects effects Interaction	Between subjects effects Genotype	Between subjects effects Sex
	n=10	n=10	n=12	n=10			
Cortical Area (mm^2)	0.82 (0.03)[a]	0.58 (0.02)[b]	0.71 (0.03)[c]	0.56 (0.02)[b]	p=0.091 [η_p^2=0.074]	p<0.001 [η_p^2=0.566]	p=0.026 [η_p^2=0.124]
Cortical Thickness (mm)	0.19 (0.005)[a]	0.15 (0.003)[b]	0.17 (0.008)[a,b]	0.15 (0.007)[b]	p=0.270 [η_p^2=0.032]	p<0.001 [η_p^2=0.367]	p=0.139 [η_p^2=0.057]
Imax (mm^4)	0.27 (0.01)[a]	0.16 (0.01)[b]	0.22 (0.01)[c]	0.15 (0.01)[b]	p=0.075 [η_p^2=0.081]	p<0.001 [η_p^2=0.585]	p=0.019 [η_p^2=0.137]
Imin (mm^4)	0.15 (0.01)[a]	0.08 (0.004)[b]	0.12 (0.005)[c]	0.08 (0.003)[b]	p=0.004 [η_p^2=0.202]	p<0.001 [η_p^2=0.740]	p=0.001 [η_p^2=0.253]
TMD (g/cm^3 HA)	1.05 (0.01)[a]	0.99 (0.01)[b]	1.05 (0.02)[a]	1.01 (0.02)[a,b]	p=0.655 [η_p^2=0.005]	p=0.001 [η_p^2=0.253]	p=0.592 [η_p^2=0.008]
	Male Control 16 Weeks	Male Dp1Tyb 16 Weeks	Female Control 16 Weeks	Female Dp1Tyb 16 Weeks			
	n=13	n=12	n=20	n=22			
Cortical Area (mm^2)	1.09 (0.02)[e]	0.92 (0.02)[f]	0.89 (0.01)[f]	0.82 (0.01)[g]	p=0.005 [η_p^2=0.130]	p<0.001 [η_p^2=0.476]	p<0.001 [η_p^2=0.585]
Cortical Thickness (mm)	0.24 (0.003)[e]	0.24 (0.004)[e]	0.22 (0.002)[f]	0.22 (0.002)[f]	p=0.184 [η_p^2=0.0.30]	p=0.136 [η_p^2=0.038]	p<0.001 [η_p^2=0.341]
Imax (mm^4)	0.43 (0.02)[e]	0.29 (0.02)[f]	0.26 (0.01)[f]	0.21 (0.01)[g]	p=0.001 [η_p^2=0.189]	p<0.001 [η_p^2=0.543]	p<0.001 [η_p^2=0.681]
Imin (mm^4)[e,h]	0.20 (0.01)[e]	0.12 (0.005)[f,g]	0.13 (0.004)[f]	0.11 (0.004)[g]	p<0.001 [η_p^2=0.241]	p<0.001 [η_p^2=0.609]	p<0.001 [η_p^2=0.452]
TMD (g/cm^3 HA)	1.14 (0.02)	1.14 (0.03)	1.15 (0.02)	1.17 (0.02)	p=0.733 [η_p^2=0.002]	p=0.889 [η_p^2=0.000]	p=0.573 [η_p^2=0.006]

Values are averages (SEM). Similarities and differences between individual groups as determined from Tukey's multiple comparisons post hoc tests; values with the same superscript letter are not significantly different. Letters a,b,c,d are used for comparisons of 6 week old animals; letters e,f,g,h are used for comparisons of 16 week old animals. Data without letters within a single row are not significantly different from each other. Subject effects are p values and partial eta squared (η_p^2) in brackets.

Table 2: Mechanical Testing at 6 weeks

	Male Control 6 Week	Male Dp1Tyb 6 Week	Female Control 6 Week	Female Dp1Tyb 6 week	Between subjects effects Interaction	Between subjects effects Genotype	Between subjects effects Sex
	n=10	n=10	n=12	n=10			
Yield Force (N)	6.53 (0.68)	5.26 (0.52)	6.92 (1.08)	4.95 (0.54)	p=0.663 [η_p^2=0.005]	p=0.048 [η_p^2=0.099]	p=0.958 [η_p^2=0.000]
Ultimate Force (N)	12.90 (0.71)[a]	7.87 (0.34)[b]	10.30 (0.77)[c]	7.51 (0.51)[b]	p=0.083 [η_p^2=0.077]	p<0.001 [η_p^2=0.503]	p=0.024 [η_p^2=0.127]
Displacement to Yield (µm)	104.40 (10.71)	139.10 (13.51)	149.08 (26.28)	150.0 (25.78)	p=0.430 [η_p^2=0.016]	p=0.405 [η_p^2=0.018]	p=0.197 [η_p^2=0.043]
Postyield Displacement (µm)	481.80 (22.66)	464.70 (38.43)	487.42 (32.24)	664.60 (176.05)	p=0.279 [η_p^2=0.031]	p=0.371 [η_p^2=0.021]	p=0.253 [η_p^2=0.034]
Total Displacement (µm)	586.20 (20.94)	603.80 (36.62)	636.50 (26.11)	814.60 (171.38)	p=0.353 [η_p^2=0.023]	p=0.259 [η_p^2=0.033]	p=0.135 [η_p^2=0.058]
Stiffness (N/mm)	76.81 (5.58)[a]	43.28 (2.42)[b]	55.26 (3.36)[b]	45.13 (8.23)[b]	p=0.032 [η_p^2=0.116]	p<0.001 [η_p^2=0.313]	p=0.068 [η_p^2=0.085]
Work to Yield (mJ)	0.40 (0.07)	0.44 (0.09)	0.79 (0.26)	0.49 (0.14)	p=0.332 [η_p^2=0.025]	p=0.463 [η_p^2=0.014]	p=0.208 [η_p^2=0.041]
Postyield Work (mJ)	5.39 (0.34)[a]	3.25 (0.29)[b]	4.31 (0.37)[a,b]	3.55 (0.47)[b]	p=0.072 [η_p^2=0.083]	p<0.001 [η_p^2=0.281]	p=0.306 [η_p^2=0.028]
Total Work (mJ)	5.79 (0.35)[a]	3.69 (0.28)[b]	5.09 (0.51)[a,b]	4.04 (0.46)[b]	p=0.223 [η_p^2=0.039]	p=0.001 [η_p^2=0.267]	p=0.693 [η_p^2=0.004]
Yield Stress (MPa)	58.02 (6.09)	76.45 (7.79)	69.84 (6.93)	72.97 (7.39)	p=0.289 [η_p^2=0.030]	p=0.138 [η_p^2=0.057]	p=0.561 [η_p^2=0.009]
Ultimate Stress (MPa)	112.41 (2.44)	113.16 (4.09)	108.19 (3.67)	109.74 (3.54)	p=0.911 [η_p^2=0.000]	p=0.746 [η_p^2=0.003]	p=0.286 [η_p^2=0.030]

Values are averages (SEM). Similarities and differences between individual groups as determined from Tukey's multiple comparisons post hoc tests; values with the same superscript letter are not significantly different. Data without letters within a single row are not significantly different from each other. Subject effects are p values and partial eta squared (η_p^2) in brackets.

Table 3: Mechanical testing at 16 week

	Male Control 16 Week	Male Dp1Tyb 16 Week	Female Control 16 Week	Female Dp1Tyb 16 week	Between subjects effects Interaction	Between subjects effects Genotype	Between subjects effects Sex
	n=13	n=12	n=20	n=22			
Yield Force (N)	11.30 (0.70)	11.19 (0.61)	9.42 (0.55)	11.14 (0.59)	p=0.158 [η_p^2=0.034]	p=0.211 [η_p^2=0.027]	p=0.134 [η_p^2=0.038]
Ultimate Force (N)	19.34 (0.58)^{e}	14.98 (0.52)^{f}	13.75 (0.30)^{f,g}	12.98 (0.37)^{g}	p<0.001 [η_p^2=0.231]	p<0.001 [η_p^2=0.379]	p<0.001 [η_p^2=0.572]
Displacement to Yield (µm)	123.46 (7.69)^{e}	154.82 (11.22)^{e,f}	133.18 (8.41)^{e}	177.06 (12.29)^{f}	p=0.552 [η_p^2=0.006]	p=0.001 [η_p^2=0.182]	p=0.132 [η_p^2=0.039]
Postyield Displacement (µm)	641.54 (43.80)	579.64 (93.59)	660.32 (79.03)	416.94 (50.45)	p=0.233 [η_p^2=0.024]	p=0.047 [η_p^2=0.066]	p=0.343 [η_p^2=0.016]
Total Displacement (µm)	765.00 (42.51)	734.45 (86.39)	793.50 (79.51)	594.00 (44.07)	p=0.252 [η_p^2=0.023]	p=0.121 [η_p^2=0.041]	p=0.447 [η_p^2=0.010]
Stiffness (N/mm)	102.79 (4.79)^{e}	82.66 (2.88)^{f}	82.45 (3.92)^{f}	70.22 (2.99)^{f}	p=0.333 [η_p^2=0.016]	p<0.001 [η_p^2=0.217]	p<0.001 [η_p^2=0.221]
Work to Yield (mJ)	0.82 (0.10)^{e,f}	0.99 (0.15)^{e,f}	0.74 (0.08)^{e}	1.13 (0.13)^{f}	p=0.335 [η_p^2=0.016]	p=0.021 [η_p^2=0.088]	p=0.813 [η_p^2=0.001]

Values are averages (SEM). Similarities and differences between individual groups as determined from Tukey's multiple comparisons post hoc tests; values with the same superscript letter are not significantly different. Data without letters within a single row are not significantly different from each other. Subject effects are p values and partial eta squared (η_p^2) in brackets

APPENDIX B. DYRK1A GENETIC DOSAGE IN OSTEOBLAST IN FEMALE TS65DN,*DYRK1A* MICE

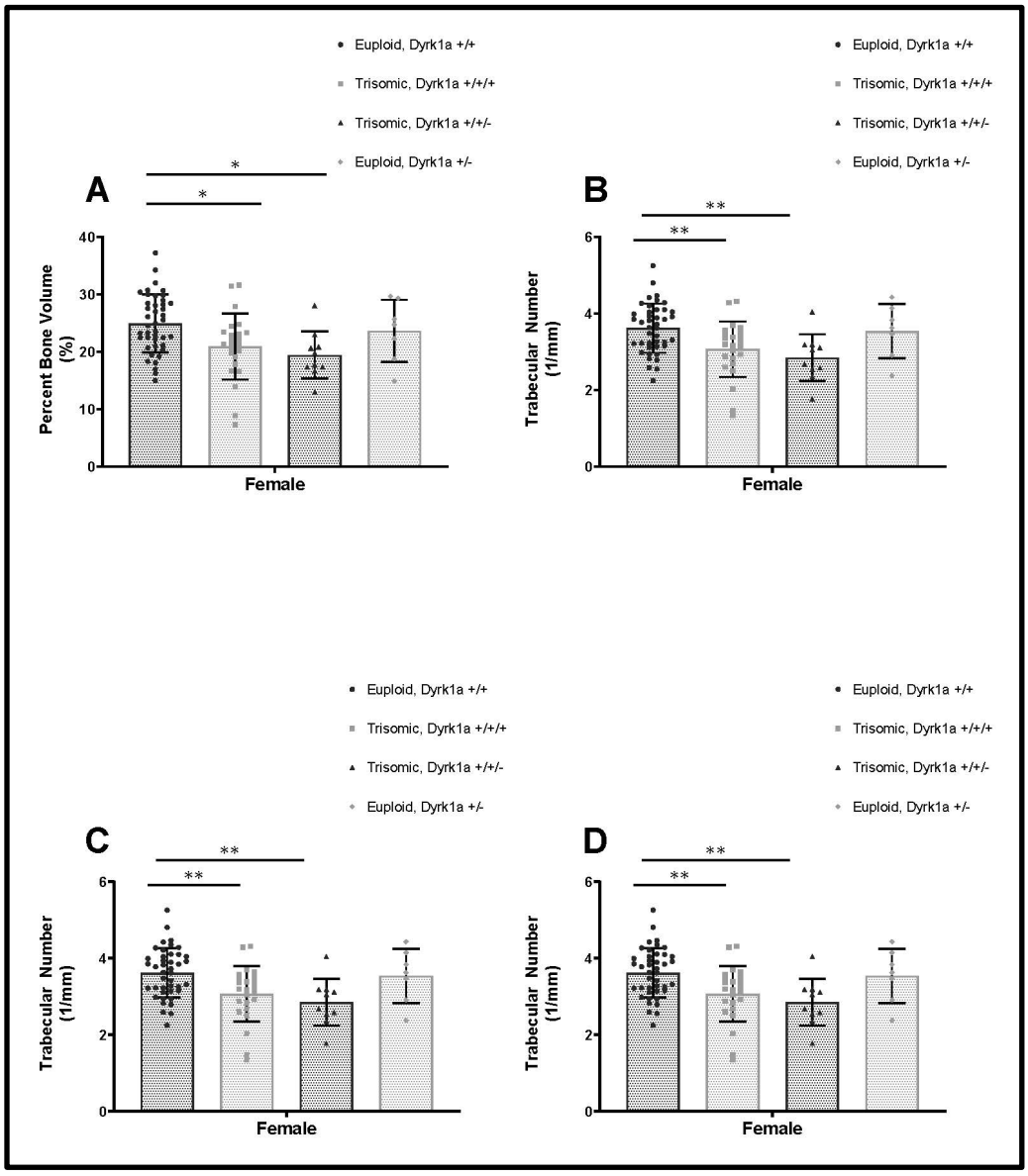

Figure 6 – Trabecular measure for six week female animals. Error bars (+/- SD). One-way ANOVA performed on trabecular parameters indicated significant effects of genotype. (A) Percent Bone Volume; (B) Trabecular Separation; (C) Trabecular Number; (D) Trabecular Thickness. Female Euploid,*Dyrk1a*$^{+/+}$ (n=42); Trisomic,*Dyrk1a*$^{+/+/+}$ (n=24); Trisomic,*Dyrk1a*$^{+/+/-}$ (n=10); Euploid,*Dyrk1a*$^{+/-}$ (n=7). Similarities and differences between individual groups are determined from Tukey's multiple comparisons post hoc tests. (*, $p<0.05$; **, $p<0.005$, ***, $p<0.0002$, ****, $p<0.0001$)

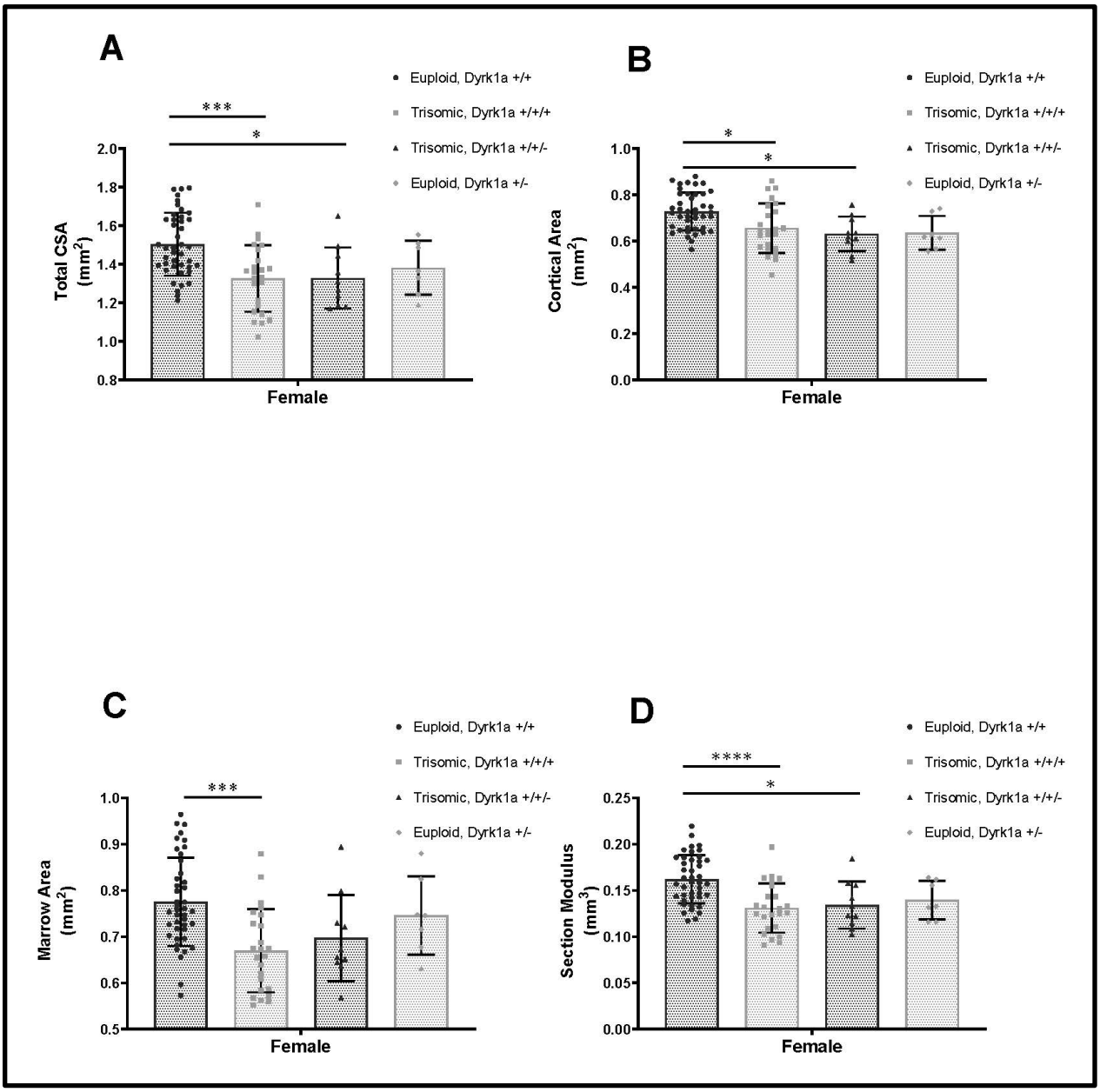

Figure 7 – Cortical measures on female euploid and trisomic femurs at 6 weeks of age. Error bars (+/- SD). One-way ANOVA was used to determine significant differences between genotypes. (A) Total CSA; (B) Cortical area; (C) Marrow Area; (D) Section Modulus. Trisomic,*Dyrk1a*$^{+/+/+}$ and Trisomic,*Dyrk1a*$^{+/+/-}$ animals had significant deficits in Total CSA, Cortical Area, and Section Modulus. Only Trisomic,*Dyrk1a*$^{+/+/+}$ exhibited deficits in Marrow Area. . (*, $p<0.05$; **, $p<0.005$, ***, $p<0.0002$, ****, $p<0.0001$)

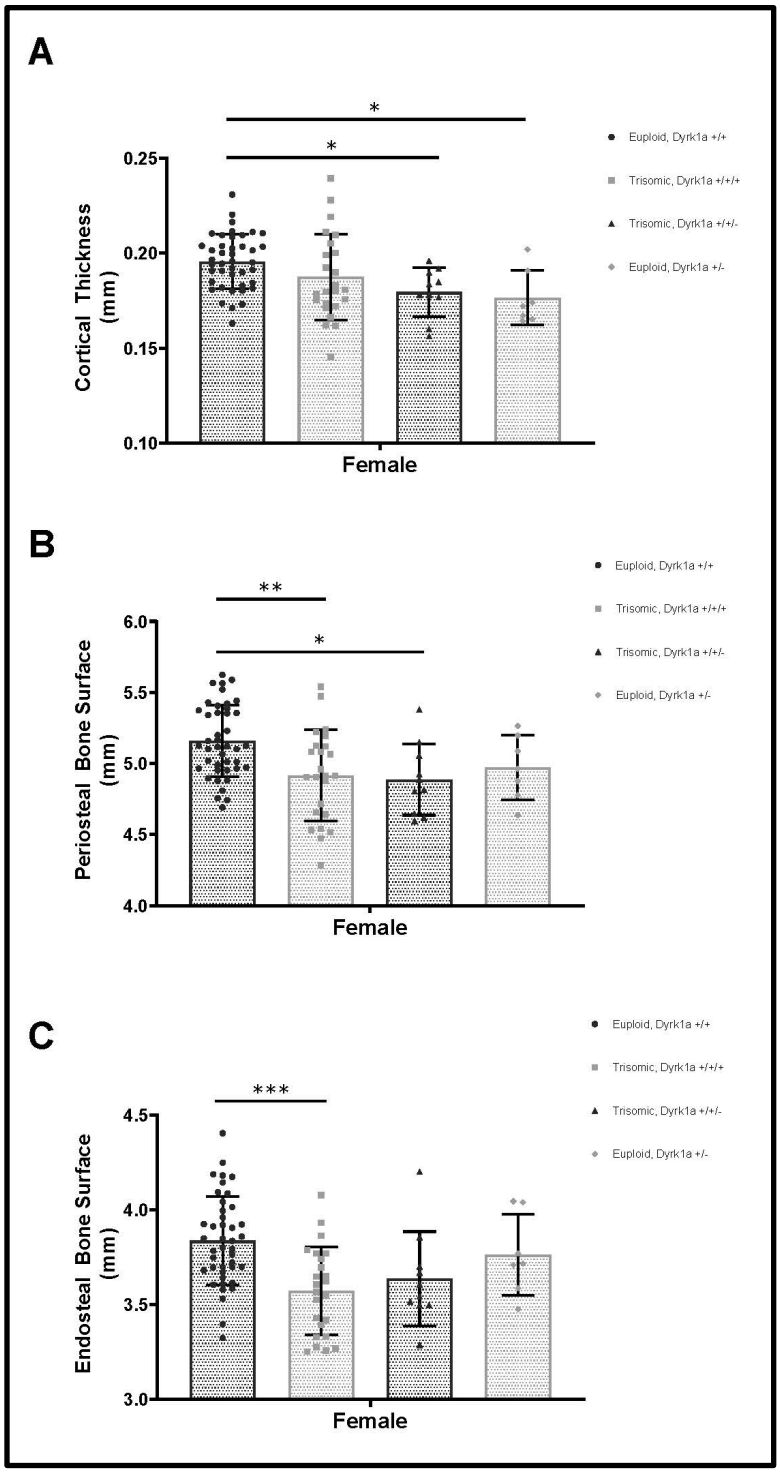

Figure 8 - Cortical measures on female euploid and trisomic femurs at 6 weeks of age. Error bars (+/- SD). One-way ANOVA was used to determine significant differences between genotypes. (A) Cortical Thickness; (B) Periosteal Bone Surface; (C) Endosteal Bone Surface. Euploid,*Dyrk1a*$^{+/+}$ had increased Cortical Thickness, Ps.BS, and Es.BS compared to Trisomic,*Dyrk1a*$^{+/+/+}$ animals. No differences were observed between any other genotypes. (*, $p<0.05$; **, $p<0.005$, ***, $p<0.0002$, ****, $p<0.0001$)

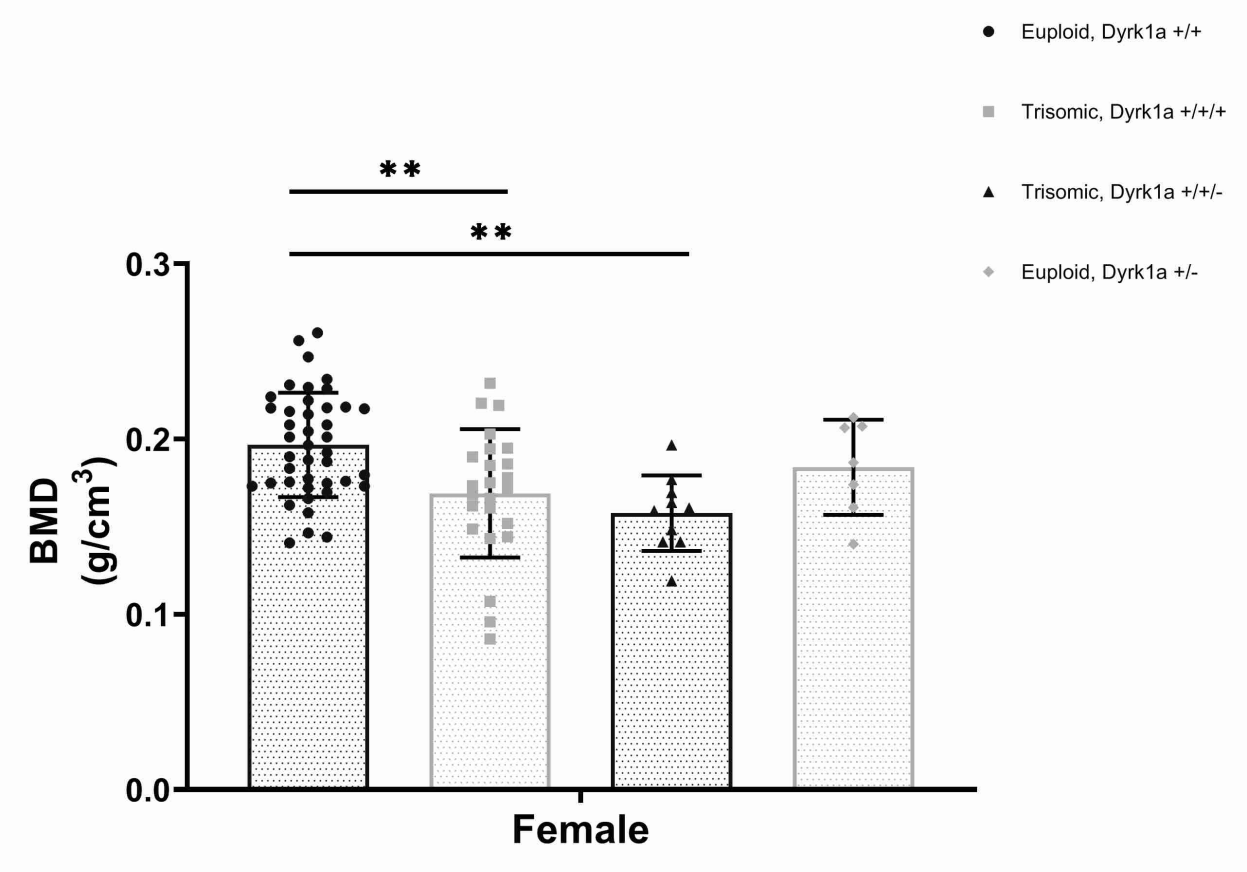

Figure 9 – BMD of female Ts65Dn mice. One-way ANOVA was used to determine significant differences between genotypes. Trisomic,*Dyrk1a*$^{+/+/+}$ and *Dyrk1a*$^{+/+/-}$ mice lower BMD compared to euploid controls. (*, p<0.05; **, p<0.005, ***, p<0.0002, ****, p<0.0001)

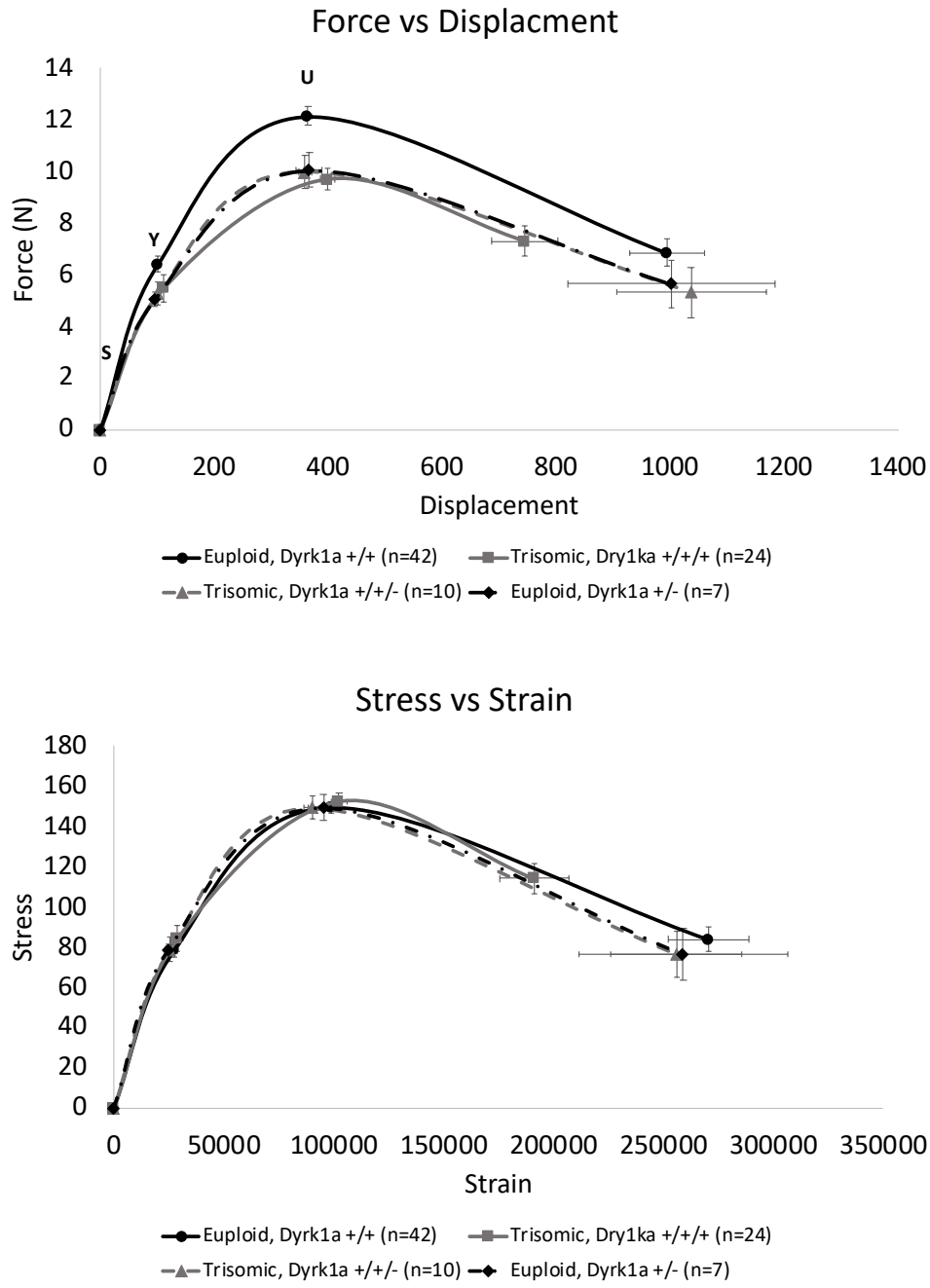

Figure 10 - Schematic representation of mechanical testing curves (data represented by mean ± SEM). A and B) Representations of force-displacement curves at the structural level. C and D) Representations of stress-strain curves at the tissue level. S, is related to the stiffness or modulus of the femur. Y, the yield point represents elastic behavior, indicating the bone's resistance to permanent deformation, past this point, U is the plastic region or permanent deformation where the bone has sustained permanent damage.

Table 4 - Cortical Architecture and Geometry of 6 week Female Ts65Dn mice

	Euploid, Dyrk1a +/+ (n=42)	**Trisomic, Dyrk1a +/+/+ (n=24)**	**Trisomic, Dyrk1a +/+/- (n=10)**	**Euploid, Dyrk1a +/- (n=7)**
Imax (mm^4)	0.1797 (0.0062)	0.1521 (0.0095)*	0.1397 (0.0103)*	0.1436 (0.0110)
Theta max (deg)	59.9787 (12.3217)	81.0503 (17.6908)	21.9311 (17.2666)	54.5954 (31.8023)
Imin (mm^4)	0.0990 (0.0033)	0.0741 (0.0039)****	0.0757 (0.0061)**	0.0816 (0.0064)
Theta min (deg)	93.0400 (0.7545)	90.6932 (0.7727)	93.9311 (1.3153)	93.1669 (1.9002)
AP Width (mm)	1.1921 (0.0105)	1.0983 (0.0136)****	1.1185 (0.0217)*	1.1520 (0.0264)
ML Width (mm)	1.6340 (0.0151)	1.5765 (0.0291)	1.5392 (0.0289)	1.5634 (0.0281)
AP/ML	0.7306 (0.0056)	0.7002 (0.0109)*	0.7273 (0.0104)	0.7370 (0.0114)
Iap (mm^4)	0.1789 (0.0061)	0.1517 (0.0094)*	0.1390 (0.0103)*	0.1430 (0.0110)
Iml (mm^4)	0.0998 (0.0033)	0.0744 (0.0040)****	0.0763 (0.0061)**	0.0822 (0.0065)
Medial Extreme (mm)	0.8136 (0.0080)	0.7705 (0.0143)*	0.7531 (0.0150)*	0.7751 (0.0148)
TMD (g/cm^3 HA)	1.0808 (0.0049)	1.0592 (0.0063)*	1.0607 (0.0095)	1.0722 (0.0119)

Values are averages (SEM). Similarities and differences between individual groups as determined from Tukey's multiple comparisons post hoc tests; values with the asterisks denote significance compared to euploid animals. (*, $p<0.05$; **, $p<0.005$, ***, $p<0.0002$, ****, $p<0.0001$)

Table 5 – Mechanical Testing of 6 week female mice

	Euploid, Dyrk1a +/+ (n=42)	**Trisomic, Dyrk1a +/+/+ (n=24)**	**Trisomic, Dyrk1a +/+/- (n=10)**	**Euploid, Dyrk1a +/- (n=7)**
Yield Force (N)	6.4055 (0.3216)	5.4721 (0.5445)	5.2549 (0.4460)	5.0477 (0.2896)
Ultimate Force (N)	12.1269 (0.3626)	9.6960 (0.4306)***	9.9729 (0.6287)*	10.0440 (0.6642)
Displacement to Yield (µm)	101.2621 (4.5441)	111.7288 (8.0270)	101.7181 (3.7311)	95.8871 (3.8492)
Postyield Displacement (µm)	893.7143 (64.9399)	633.5000 (62.9873)	935.2000 (130.6428)	906.5714 (180.0648)
Total Displacment (µm)	994.9764 (65.6901)	745.2288 (58.5828)	1036.9181 (131.2504)	1002.4585 (182.6172)
Stiffness (N/mm)	143.0620 (55.7021)	160.4556 (108.7069)	55.8269 (3.4068)	57.7634 (3.4224)
Work to Yield (mJ)	0.3689 (0.0296)	0.3718 (0.0641)	0.2882 (0.0337)	0.2560 (0.0205)
Postyield Work (mJ)	7.6203 (0.4818)	4.9159 (0.4266)**	6.3510 (0.6808)	6.1641 (1.0639)
Total Work (mJ)	7.9892 (0.4931)	5.2877 (0.4111)**	6.6391 (0.6956)	6.4200 (1.0807)
Yield Stress (MPa)	78.3212 (3.2659)	84.1241 (6.3764)	78.7097 (5.9132)	72.3590 (2.7426)
Ultimate Stress (MPa)	149.4028 (2.4714)	152.4522 (3.9217)	149.2933 (5.7450)	143.6495 (6.2807)
Strain to Yield (µe)	27456.2989 (1270.3358)	28901.1096 (2278.7009)	25495.0868 (931.8943)	24762.7929 (1057.0592)
Total Strain (µe)	270627.4809 (18203.2581)	191300.3102 (15719.7649)*	255988.7176 (29761.2341)	258922.9442 (47307.3855)
Modulus (GPa)	7.2620 (3.1469)	9.6710 (6.5047)	3.3507 (0.1593)	3.2000 (0.1023)
Resilience (MPa)	1.2195 (0.0911)	1.4581 (0.2151)	1.0792 (0.1196)	0.9494 (0.0657)
Toughness (MPa)	26.8858 (1.5688)	21.7338 (1.5571)	25.3643 (2.8536)	23.6593 (3.6110)
Failure Force (N)	6.8442 (0.5397)	7.3028 (0.5929)	5.3142 (0.9842)	5.6381 (0.9422)
Ultimate Displacement (µm)	364.5478 (7.5229)	399.0205 (12.5666)	359.4181 (12.0304)	367.0299 (22.6065)
Failure Stress (MPa)	83.7562 (5.9275)	113.9926 (7.5441)*	76.4849 (11.2289)	80.1114 (12.8767)*
Ultimate Strain (µe)	98970.1673 (2387.2733)	102398.7124 (3636.3700)	90449.9640 (4232.6065)	95276.4840 (7082.4633)

Values are averages (SEM). Similarities and differences between individual groups as determined from Tukey's multiple comparisons post hoc tests; values with the asterisks denote significance compared to euploid animals. (*, $p<0.05$; **, $p<0.005$, ***, $p<0.0002$, ****, $p<0.0001$)

Table 6 – Postnatal Death of Ts65Dn

Age at Death	Sex	Ts 3 copies	Ts 2 copies	Eu 2 copies	Eu 1 copy	Total
Aborted	Male	4		2		6
	Female	3		1		4
1 Day	Male	6		7	1	9
	Female	4		6		10
2 Days	Male		1	2	1	4
	Female					
14-36 days	Male	2	1	1		4
	Female			2		2
Totals		19	2	21	2	44

Values are the total number mice that have perished separated by their copy number of *Dyrk1a*. A total of 2 trisomic males with reduced copy number of *Dyrk1a* died before P42.

REFERENCES

Abekhoukh, S., Planque, C., Ripoll, C., Urbaniak, P., Paul, J. L., Delabar, J. M., & Janel, N. (2013). Dyrk1A, a serine/threonine kinase, is involved in ERK and Akt activation in the brain of hyperhomocysteinemic mice. *Mol Neurobiol, 47*(1), 105-116. doi:10.1007/s12035-012-8326-1

Abeysekera, I., Thomas, J., Georgiadis, T. M., Berman, A. G., Hammond, M. A., Dria, K. J., . . . Roper, R. J. (2016). Differential effects of Epigallocatechin-3-gallate containing supplements on correcting skeletal defects in a Down syndrome mouse model. *Mol Nutr Food Res, 60*(4), 717-726. doi:10.1002/mnfr.201500781

Amano, K., Sago, H., Uchikawa, C., Suzuki, T., Kotliarova, S. E., Nukina, N., . . . Yamakawa, K. (2004). Dosage-dependent over-expression of genes in the trisomic region of Ts1Cje mouse model for Down syndrome. *Hum Mol Genet, 13*(13), 1333-1340. doi:10.1093/hmg/ddh154

Angelopoulou, N., Matziari, C., Tsimaras, V., Sakadamis, A., Souftas, V., & Mandroukas, K. (2000). Bone mineral density and muscle strength in young men with mental retardation (with and without Down syndrome). *Calcif Tissue Int, 66*(3), 176-180.

Angelopoulou, N., Souftas, V., Sakadamis, A., & Mandroukas, K. (1999). Bone mineral density in adults with Down's syndrome. *Eur Radiol, 9*(4), 648-651. doi:10.1007/s003300050726

Antonarakis, S. E., Lyle, R., Dermitzakis, E. T., Reymond, A., & Deutsch, S. (2004). Chromosome 21 and down syndrome: from genomics to pathophysiology. *Nat Rev Genet, 5*(10), 725-738. doi:10.1038/nrg1448

Arron, J. R., Winslow, M. M., Polleri, A., Chang, C. P., Wu, H., Gao, X., . . . Crabtree, G. R. (2006). NFAT dysregulation by increased dosage of DSCR1 and DYRK1A on chromosome 21. *Nature, 441*(7093), 595-600. doi:10.1038/nature04678

Baek, K. H., Zaslavsky, A., Lynch, R. C., Britt, C., Okada, Y., Siarey, R. J., . . . Ryeom, S. (2009). Down's syndrome suppression of tumour growth and the role of the calcineurin inhibitor DSCR1. *Nature, 459*(7250), 1126-1130. doi:10.1038/nature08062

Baird, P. A., & Sadovnick, A. D. (1989). Life tables for Down syndrome. *Hum Genet, 82*(3), 291-292.

Baptista, F., Varela, A., & Sardinha, L. B. (2005). Bone mineral mass in males and females with and without Down syndrome. *Osteoporos Int, 16*(4), 380-388. doi:10.1007/s00198-004-1687-1

Barnhart, R. C., & Connolly, B. (2007). Aging and Down syndrome: implications for physical therapy. *Phys Ther, 87*(10), 1399-1406. doi:10.2522/ptj.20060334

Baxter, L. L., Moran, T. H., Richtsmeier, J. T., Troncoso, J., & Reeves, R. H. (2000). Discovery and genetic localization of Down syndrome cerebellar phenotypes using the Ts65Dn mouse. *Hum Mol Genet, 9*(2), 195-202.

Baxter-Jones, A. D., Faulkner, R. A., Forwood, M. R., Mirwald, R. L., & Bailey, D. A. (2011). Bone mineral accrual from 8 to 30 years of age: an estimation of peak bone mass. *J Bone Miner Res, 26*(8), 1729-1739. doi:10.1002/jbmr.412

Bellido, T., Plotkin, L., & Bruzzaniti, A. (2013). Bone Cells. In D. B. A. Burr, M. R. (Ed.), *Basic and Applied Bone Biology* (pp. 27-45): Elsevier Inc.

Berman, A. G., Clauser, C. A., Wunderlin, C., Hammond, M. A., & Wallace, J. M. (2015). Structural and Mechanical Improvements to Bone Are Strain Dependent with Axial

Compression of the Tibia in Female C57BL/6 Mice. *PLoS One, 10*(6), e0130504. doi:10.1371/journal.pone.0130504

Bittles, A. H., & Glasson, E. J. (2004). Clinical, social, and ethical implications of changing life expectancy in Down syndrome. *Dev Med Child Neurol, 46*(4), 282-286.

Blazek, J. D., Abeysekera, I., Li, J., & Roper, R. J. (2015). Rescue of the abnormal skeletal phenotype in Ts65Dn Down syndrome mice using genetic and therapeutic modulation of trisomic Dyrk1a. *Hum Mol Genet, 24*(20), 5687-5696. doi:10.1093/hmg/ddv284

Blazek, J. D., Gaddy, A., Meyer, R., Roper, R. J., & Li, J. (2011). Disruption of bone development and homeostasis by trisomy in Ts65Dn Down syndrome mice. *Bone, 48*(2), 275-280. doi:10.1016/j.bone.2010.09.028

Blazek, J. D., Malik, A. M., Tischbein, M., Arbones, M. L., Moore, C. S., & Roper, R. J. (2015). Abnormal mineralization of the Ts65Dn Down syndrome mouse appendicular skeleton begins during embryonic development in a Dyrk1a-independent manner. *Mech Dev, 136*, 133-142. doi:10.1016/j.mod.2014.12.004

Bonewald, L. F. (2011). The amazing osteocyte. *J Bone Miner Res, 26*(2), 229-238. doi:10.1002/jbmr.320

Bromley, B., Lieberman, E., Shipp, T. D., & Benacerraf, B. R. (2002a). Fetal nose bone length: a marker for Down syndrome in the second trimester. *J Ultrasound Med, 21*(12), 1387-1394.

Bromley, B., Lieberman, E., Shipp, T. D., & Benacerraf, B. R. (2002b). The genetic sonogram: a method of risk assessment for Down syndrome in the second trimester. *J Ultrasound Med, 21*(10), 1087-1096; quiz 1097-1088.

Burr, D. B., & Akkus, O. (2014). Bone Morphology and Organization In D. B. A. Burr, M. R. (Ed.), *Basic and Applied Bone Biology* (pp. 3-25): Elsevier Inc.

Burr, D. B., & Allen, M. R. (2014). Bone Modeling and Remodeling. In D. B. A. Burr, M. R. (Ed.), *Basic and Applied Bone Biology* (pp. 75-90): Elsevier.

Carfi, A., Liperoti, R., Fusco, D., Giovannini, S., Brandi, V., Vetrano, D. L., . . . Onder, G. (2017). Bone mineral density in adults with Down syndrome. *Osteoporos Int, 28*(10), 2929-2934. doi:10.1007/s00198-017-4133-x

Center, J., Beange, H., & McElduff, A. (1998). People with mental retardation have an increased prevalence of osteoporosis: a population study. *Am J Ment Retard, 103*(1), 19-28. doi:10.1352/0895-8017(1998)103<0019:PWMRHA>2.0.CO;2

Chakrabarti, L., Best, T. K., Cramer, N. P., Carney, R. S., Isaac, J. T., Galdzicki, Z., & Haydar, T. F. (2010). Olig1 and Olig2 triplication causes developmental brain defects in Down syndrome. *Nat Neurosci, 13*(8), 927-934. doi:10.1038/nn.2600

Chaney, R. H., & Eyman, R. K. (2000). Patterns in mortality over 60 years among persons with mental retardation in a residential facility. *Ment Retard, 38*(3), 289-293. doi:10.1352/0047-6765(2000)038<0289:PIMOYA>2.0.CO;2

Chen, J., Shi, Y., Regan, J., Karuppaiah, K., Ornitz, D. M., & Long, F. (2014). Osx-Cre targets multiple cell types besides osteoblast lineage in postnatal mice. *PLoS One, 9*(1), e85161. doi:10.1371/journal.pone.0085161

Cole, J. H., & van der Meulen, M. C. (2011). Whole bone mechanics and bone quality. *Clin Orthop Relat Res, 469*(8), 2139-2149. doi:10.1007/s11999-011-1784-3

Costa, R., De Miguel, R., Garcia, C., de Asua, D. R., Castaneda, S., Moldenhauer, F., & Suarez, C. (2017). Bone Mass Assessment in a Cohort of Adults With Down Syndrome: A Cross-Sectional Study. *Intellect Dev Disabil, 55*(5), 315-324. doi:10.1352/1934-9556-55.5.315

Costa, R., Gullon, A., De Miguel, R., de Asua, D. R., Bautista, A., Garcia, C., . . . Moldenhauer, F. (2018). Bone Mineral Density Distribution Curves in Spanish Adults With Down Syndrome. *J Clin Densitom*. doi:10.1016/j.jocd.2018.03.001

Cronk, C., Crocker, A. C., Pueschel, S. M., Shea, A. M., Zackai, E., Pickens, G., & Reed, R. B. (1988). Growth charts for children with Down syndrome: 1 month to 18 years of age. *Pediatrics, 81*(1), 102-110.

Davisson, M. T., Schmidt, C., Reeves, R. H., Irving, N. G., Akeson, E. C., Harris, B. S., & Bronson, R. T. (1993). Segmental trisomy as a mouse model for Down syndrome. *Prog Clin Biol Res, 384*, 117-133.

de Graaf, G., Buckley, F., & Skotko, B. G. (2017). Estimation of the number of people with Down syndrome in the United States. *Genet Med, 19*(4), 439-447. doi:10.1038/gim.2016.127

de Moraes, M. E., Tanaka, J. L., de Moraes, L. C., Filho, E. M., & de Melo Castilho, J. C. (2008). Skeletal age of individuals with Down syndrome. *Spec Care Dentist, 28*(3), 101-106. doi:10.1111/j.1754-4505.2008.00020.x

Deitz, S. L., Blazek, J. D., Solzak, J. P., & Roper, R. J. (2011). Down Syndrome: A Complex and Interactive Genetic Disorder. *Genetics and Etiology of Down Syndrome*. doi:10.5772/18436

Deitz, S. L., & Roper, R. J. (2011). Trisomic and allelic differences influence phenotypic variability during development of Down syndrome mice. *Genetics, 189*(4), 1487-1495. doi:10.1534/genetics.111.131391

Delabar, J. M., Theophile, D., Rahmani, Z., Chettouh, Z., Blouin, J. L., Prieur, M., . . . Sinet, P. M. (1993). Molecular mapping of twenty-four features of Down syndrome on chromosome 21. *Eur J Hum Genet, 1*(2), 114-124. doi:10.1159/000472398

Down, J. L. (1995). Observations on an ethnic classification of idiots. 1866. *Ment Retard, 33*(1), 54-56.

Dreyfus, D., Lauer, E., & Wilkinson, J. (2014). Characteristics associated with bone mineral density screening in adults with intellectual disabilities. *J Am Board Fam Med, 27*(1), 104-114. doi:10.3122/jabfm.2014.01.130114

Duchon, A., Raveau, M., Chevalier, C., Nalesso, V., Sharp, A. J., & Herault, Y. (2011). Identification of the translocation breakpoints in the Ts65Dn and Ts1Cje mouse lines: relevance for modeling Down syndrome. *Mamm Genome, 22*(11-12), 674-684. doi:10.1007/s00335-011-9356-0

Epstein, C. J. (2014). Down Syndrome (Trisomy 21). In A. L. Beaudet, B. Vogelstein, K. W. Kinzler, S. E. Antonarakis, A. Ballabio, K. M. Gibson, & G. Mitchell (Eds.), *The Online Metabolic and Molecular Bases of Inherited Disease*. New York, NY: The McGraw-Hill Companies, Inc.

Esbensen, A. J. (2010). Health conditions associated with aging and end of life of adults with Down syndrome. *Int Rev Res Ment Retard, 39*(C), 107-126. doi:10.1016/S0074-7750(10)39004-5

Esquirol, J. E. t. D., & Hunt, E. K. (1845). *Mental maladies. A treatise on insanity*. Philadelphia,: Lea and Blanchard.

Florencio-Silva, R., Sasso, G. R., Sasso-Cerri, E., Simoes, M. J., & Cerri, P. S. (2015). Biology of Bone Tissue: Structure, Function, and Factors That Influence Bone Cells. *Biomed Res Int, 2015*, 421746. doi:10.1155/2015/421746

Fonseca, H., Moreira-Goncalves, D., Coriolano, H. J., & Duarte, J. A. (2014). Bone quality: the determinants of bone strength and fragility. *Sports Med, 44*(1), 37-53. doi:10.1007/s40279-013-0100-7

Fotaki, V., Dierssen, M., Alcantara, S., Martinez, S., Marti, E., Casas, C., . . . Arbones, M. L. (2002). Dyrk1A haploinsufficiency affects viability and causes developmental delay and abnormal brain morphology in mice. *Mol Cell Biol, 22*(18), 6636-6647.

Fowler, T. W., McKelvey, K. D., Akel, N. S., Vander Schilden, J., Bacon, A. W., Bracey, J. W., . . . Suva, L. J. (2012). Low bone turnover and low BMD in Down syndrome: effect of intermittent PTH treatment. *PLoS One, 7*(8), e42967. doi:10.1371/journal.pone.0042967

Gardiner, K. (2004). Gene-dosage effects in Down syndrome and trisomic mouse models. *Genome Biol, 5*(10), 244. doi:10.1186/gb-2004-5-10-244

Gardiner, K. J. (2010). Molecular basis of pharmacotherapies for cognition in Down syndrome. *Trends Pharmacol Sci, 31*(2), 66-73. doi:10.1016/j.tips.2009.10.010

Garnero, P. (2015). The Role of Collagen Organization on the Properties of Bone. *Calcif Tissue Int, 97*(3), 229-240. doi:10.1007/s00223-015-9996-2

Geijer, J. R., Stanish, H. I., Draheim, C. C., & Dengel, D. R. (2014). Bone mineral density in adults with Down syndrome, intellectual disability, and nondisabled adults. *Am J Intellect Dev Disabil, 119*(2), 107-114. doi:10.1352/1944-7558-119.2.107

Gonzalez-Aguero, A., Vicente-Rodriguez, G., Gomez-Cabello, A., & Casajus, J. A. (2013). Cortical and trabecular bone at the radius and tibia in male and female adolescents with Down syndrome: a peripheral quantitative computed tomography (pQCT) study. *Osteoporos Int, 24*(3), 1035-1044. doi:10.1007/s00198-012-2041-7

Gonzalez-Aguero, A., Vicente-Rodriguez, G., Moreno, L. A., & Casajus, J. A. (2011). Bone mass in male and female children and adolescents with Down syndrome. *Osteoporos Int, 22*(7), 2151-2157. doi:10.1007/s00198-010-1443-7

Gupta, M., Dhanasekaran, A. R., & Gardiner, K. J. (2016). Mouse models of Down syndrome: gene content and consequences. *Mamm Genome, 27*(11-12), 538-555. doi:10.1007/s00335-016-9661-8

Hawli, Y., Nasrallah, M., & El-Hajj Fuleihan, G. (2009). Endocrine and musculoskeletal abnormalities in patients with Down syndrome. *Nat Rev Endocrinol, 5*(6), 327-334. doi:10.1038/nrendo.2009.80

He, Y., Staser, K., Rhodes, S. D., Liu, Y., Wu, X., Park, S. J., . . . Yang, F. C. (2011). Erk1 positively regulates osteoclast differentiation and bone resorptive activity. *PLoS One, 6*(9), e24780. doi:10.1371/journal.pone.0024780

Hernandez, D., & Fisher, E. M. (1996). Down syndrome genetics: unravelling a multifactorial disorder. *Hum Mol Genet, 5 Spec No*, 1411-1416. doi:10.1093/hmg/5.supplement_1.1411

Holtzman, D. M., Santucci, D., Kilbridge, J., Chua-Couzens, J., Fontana, D. J., Daniels, S. E., . . . Mobley, W. C. (1996). Developmental abnormalities and age-related neurodegeneration in a mouse model of Down syndrome. *Proc Natl Acad Sci U S A, 93*(23), 13333-13338.

Howard-Jones, N. (1979). On the diagnostic term "Down's disease". *Med Hist, 23*(1), 102-104. doi:10.1017/s0025727300051048

Huang, W., & Olsen, B. R. (2015). Skeletal defects in Osterix-Cre transgenic mice. *Transgenic Res, 24*(1), 167-172. doi:10.1007/s11248-014-9828-6

Insausti, A. M., Megias, M., Crespo, D., Cruz-Orive, L. M., Dierssen, M., Vallina, I. F., . . . Florez, J. (1998). Hippocampal volume and neuronal number in Ts65Dn mice: a murine model of Down syndrome. *Neurosci Lett, 253*(3), 175-178.

Jilka, R. L. (2013). The relevance of mouse models for investigating age-related bone loss in humans. *J Gerontol A Biol Sci Med Sci, 68*(10), 1209-1217. doi:10.1093/gerona/glt046

Kahlem, P., Sultan, M., Herwig, R., Steinfath, M., Balzereit, D., Eppens, B., . . . Yaspo, M. L. (2004). Transcript level alterations reflect gene dosage effects across multiple tissues in a mouse model of down syndrome. *Genome Res, 14*(7), 1258-1267. doi:10.1101/gr.1951304

Kao, C. H., Chen, C. C., Wang, S. J., & Yeh, S. H. (1992). Bone mineral density in children with Down's syndrome detected by dual photon absorptiometry. *Nucl Med Commun, 13*(10), 773-775.

Keeling, J. W., Hansen, B. F., & Kjaer, I. (1997). Pattern of malformations in the axial skeleton in human trisomy 21 fetuses. *Am J Med Genet, 68*(4), 466-471.

Korbel, J. O., Tirosh-Wagner, T., Urban, A. E., Chen, X. N., Kasowski, M., Dai, L., . . . Korenberg, J. R. (2009). The genetic architecture of Down syndrome phenotypes revealed by high-resolution analysis of human segmental trisomies. *Proc Natl Acad Sci U S A, 106*(29), 12031-12036. doi:10.1073/pnas.0813248106

Korenberg, J. R., Chen, X. N., Schipper, R., Sun, Z., Gonsky, R., Gerwehr, S., . . . et al. (1994). Down syndrome phenotypes: the consequences of chromosomal imbalance. *Proc Natl Acad Sci U S A, 91*(11), 4997-5001. doi:10.1073/pnas.91.11.4997

LaCombe, J. M., & Roper, R. J. (2020). Skeletal dynamics of Down syndrome: A developing perspective. *Bone, 133*, 115215. doi:10.1016/j.bone.2019.115215

Lana-Elola, E., Watson-Scales, S., Slender, A., Gibbins, D., Martineau, A., Douglas, C., . . . Tybulewicz, V. (2016). Genetic dissection of Down syndrome-associated congenital heart defects using a new mouse mapping panel. *Elife, 5*. doi:10.7554/eLife.11614

Lana-Elola, E., Watson-Scales, S. D., Fisher, E. M., & Tybulewicz, V. L. (2011). Down syndrome: searching for the genetic culprits. *Dis Model Mech, 4*(5), 586-595. doi:10.1242/dmm.008078

Lee, Y., Ha, J., Kim, H. J., Kim, Y. S., Chang, E. J., Song, W. J., & Kim, H. H. (2009). Negative feedback Inhibition of NFATc1 by DYRK1A regulates bone homeostasis. *J Biol Chem, 284*(48), 33343-33351. doi:10.1074/jbc.M109.042234

Longo, D., DeFigueiredo, D., Cicero, S., Sacchini, C., & Nicolaides, K. H. (2004). Femur and humerus length in trisomy 21 fetuses at 11-14 weeks of gestation. *Ultrasound Obstet Gynecol, 23*(2), 143-147. doi:10.1002/uog.970

Lyle, R., Bena, F., Gagos, S., Gehrig, C., Lopez, G., Schinzel, A., . . . Antonarakis, S. E. (2009). Genotype-phenotype correlations in Down syndrome identified by array CGH in 30 cases of partial trisomy and partial monosomy chromosome 21. *Eur J Hum Genet, 17*(4), 454-466. doi:10.1038/ejhg.2008.214

Mai, C. T., Isenburg, J. L., Canfield, M. A., Meyer, R. E., Correa, A., Alverson, C. J., . . . National Birth Defects Prevention, N. (2019). National population-based estimates for major birth defects, 2010-2014. *Birth Defects Res, 111*(18), 1420-1435. doi:10.1002/bdr2.1589

Martin, R. B., Burr, D. B., Shakey, N. A., & Fyhrie, D. P. . (2015). Mechanical Properties of Bone. In *Skeletal Tissue Mechanics* (pp. 355-422). New York: Springer Science + Business Media.

Matute-Llorente, A., Gonzalez-Aguero, A., Gomez-Cabello, A., Vicente-Rodriguez, G., & Casajus, J. A. (2013). Decreased levels of physical activity in adolescents with down syndrome are related with low bone mineral density: a cross-sectional study. *BMC Endocr Disord, 13*, 22. doi:10.1186/1472-6823-13-22

Matute-Llorente, A., Gonzalez-Aguero, A., Vicente-Rodriguez, G., Sardinha, L. B., Baptista, F., & Casajus, J. A. (2017). Physical activity and bone mineral density at the femoral neck subregions in adolescents with Down syndrome. *J Pediatr Endocrinol Metab, 30*(10), 1075-1082. doi:10.1515/jpem-2017-0024

McCormick, M. K., Schinzel, A., Petersen, M. B., Stetten, G., Driscoll, D. J., Cantu, E. S., . . . Antonarakis, S. E. (1989). Molecular genetic approach to the characterization of the "Down syndrome region" of chromosome 21. *Genomics, 5*(2), 325-331. doi:10.1016/0888-7543(89)90065-7

McKelvey, K. D., Fowler, T. W., Akel, N. S., Kelsay, J. A., Gaddy, D., Wenger, G. R., & Suva, L. J. (2013). Low bone turnover and low bone density in a cohort of adults with Down syndrome. *Osteoporos Int, 24*(4), 1333-1338. doi:10.1007/s00198-012-2109-4

Moon, J. B., Kim, J. H., Kim, K., Youn, B. U., Ko, A., Lee, S. Y., & Kim, N. (2012). Akt induces osteoclast differentiation through regulating the GSK3beta/NFATc1 signaling cascade. *J Immunol, 188*(1), 163-169. doi:10.4049/jimmunol.1101254

Myrelid, A., Gustafsson, J., Ollars, B., & Anneren, G. (2002). Growth charts for Down's syndrome from birth to 18 years of age. *Arch Dis Child, 87*(2), 97-103. doi:10.1136/adc.87.2.97

Nakashima, K., Zhou, X., Kunkel, G., Zhang, Z., Deng, J. M., Behringer, R. R., & de Crombrugghe, B. (2002). The novel zinc finger-containing transcription factor osterix is required for osteoblast differentiation and bone formation. *Cell, 108*(1), 17-29.

Niebuhr, E. (1974). Down's syndrome. The possibility of a pathogenetic segment on chromosome no. 21. *Humangenetik, 21*(1), 99-101. doi:10.1007/bf00278575

Nyberg, D. A., Souter, V. L., El-Bastawissi, A., Young, S., Luthhardt, F., & Luthy, D. A. (2001). Isolated sonographic markers for detection of fetal Down syndrome in the second trimester of pregnancy. *J Ultrasound Med, 20*(10), 1053-1063. doi:10.7863/jum.2001.20.10.1053

Olson, L. E., & Mohan, S. (2011). Bone density phenotypes in mice aneuploid for the Down syndrome critical region. *Am J Med Genet A, 155A*(10), 2436-2445. doi:10.1002/ajmg.a.34203

Olson, L. E., Richtsmeier, J. T., Leszl, J., & Reeves, R. H. (2004). A chromosome 21 critical region does not cause specific Down syndrome phenotypes. *Science, 306*(5696), 687-690. doi:10.1126/science.1098992

Olson, L. E., Roper, R. J., Sengstaken, C. L., Peterson, E. A., Aquino, V., Galdzicki, Z., . . . Reeves, R. H. (2007). Trisomy for the Down syndrome 'critical region' is necessary but not sufficient for brain phenotypes of trisomic mice. *Hum Mol Genet, 16*(7), 774-782. doi:10.1093/hmg/ddm022

Ono, T., & Nakashima, T. (2018). Recent advances in osteoclast biology. *Histochem Cell Biol, 149*(4), 325-341. doi:10.1007/s00418-018-1636-2

Parker, S. E., Mai, C. T., Canfield, M. A., Rickard, R., Wang, Y., Meyer, R. E., . . . National Birth Defects Prevention, N. (2010). Updated National Birth Prevalence estimates for selected birth defects in the United States, 2004-2006. *Birth Defects Res A Clin Mol Teratol, 88*(12), 1008-1016. doi:10.1002/bdra.20735

Parsons, T., Ryan, T. M., Reeves, R. H., & Richtsmeier, J. T. (2007). Microstructure of trabecular bone in a mouse model for Down syndrome. *Anat Rec (Hoboken), 290*(4), 414-421. doi:10.1002/ar.20494

Patterson, D. (2007). Genetic mechanisms involved in the phenotype of Down syndrome. *Ment Retard Dev Disabil Res Rev, 13*(3), 199-206. doi:10.1002/mrdd.20162

Patterson, D. (2009). Molecular genetic analysis of Down syndrome. *Hum Genet, 126*(1), 195-214. doi:10.1007/s00439-009-0696-8

Patterson, D., & Costa, A. C. (2005). Down syndrome and genetics - a case of linked histories. *Nat Rev Genet, 6*(2), 137-147. doi:10.1038/nrg1525

Plotkin, L., & Bivi, N. (2014a). Local Regulation of Bone Cell Function. In *Basic and Applied Bone Biology* (pp. 47-73): Elsevier.

Plotkin, L., & Bivi, N. (2014b). Local Regulation of Bone Cell Function In D. B. A. Burr, M. R. (Ed.), *Basic and Applied Bone Biology* (pp. 27-45): Elsevier.

Pritchard, M. A., & Kola, I. (1999). The "gene dosage effect" hypothesis versus the "amplified developmental instability" hypothesis in Down syndrome. *J Neural Transm Suppl, 57*, 293-303.

Reeves, R. H., Irving, N. G., Moran, T. H., Wohn, A., Kitt, C., Sisodia, S. S., . . . Davisson, M. T. (1995). A mouse model for Down syndrome exhibits learning and behaviour deficits. *Nat Genet, 11*(2), 177-184. doi:10.1038/ng1095-177

Reinholdt, L. G., Ding, Y., Gilbert, G. J., Czechanski, A., Solzak, J. P., Roper, R. J., . . . Davisson, M. T. (2011). Molecular characterization of the translocation breakpoints in the Down syndrome mouse model Ts65Dn. *Mamm Genome, 22*(11-12), 685-691. doi:10.1007/s00335-011-9357-z

Rho, J. Y., Kuhn-Spearing, L., & Zioupos, P. (1998). Mechanical properties and the hierarchical structure of bone. *Med Eng Phys, 20*(2), 92-102.

Richtsmeier, J. T., Baxter, L. L., & Reeves, R. H. (2000). Parallels of craniofacial maldevelopment in Down syndrome and Ts65Dn mice. *Dev Dyn, 217*(2), 137-145.

Richtsmeier, J. T., Zumwalt, A., Carlson, E. J., Epstein, C. J., & Reeves, R. H. (2002). Craniofacial phenotypes in segmentally trisomic mouse models for Down syndrome. *Am J Med Genet, 107*(4), 317-324.

Robling, A. G., Fuchs, R. K., & Burr, D. B. (2014). Mechanical Adaptation. In D. B. A. Burr, M. R. (Ed.), *Basic and Applied Bone Biology* (pp. 175-204): Elsevier.

Rodan, G. A. (1992). Introduction to bone biology. *Bone, 13 Suppl 1*, S3-6. doi:10.1016/s8756-3282(09)80003-3

Rodan, G. A. (1998). Bone homeostasis. *Proc Natl Acad Sci U S A, 95*(23), 13361-13362. doi:10.1073/pnas.95.23.13361

Rodda, S. J., & McMahon, A. P. (2006). Distinct roles for Hedgehog and canonical Wnt signaling in specification, differentiation and maintenance of osteoblast progenitors. *Development, 133*(16), 3231-3244. doi:10.1242/dev.02480

Roper, R. J., & Reeves, R. H. (2006). Understanding the basis for Down syndrome phenotypes. *PLoS Genet, 2*(3), e50. doi:10.1371/journal.pgen.0020050

Rosello, L., Torres, R., Boronat, T., Llobet, R., & Puerto, D. (2004). Osteoporosis prevalence in a Down syndrome population, measuring different parameters. *International Medical Journal on Down Syndrome, 8*(2), 18-22.

Roubertoux, P. L., & Kerdelhue, B. (2006). Trisomy 21: from chromosomes to mental retardation. *Behav Genet, 36*(3), 346-354. doi:10.1007/s10519-006-9052-0

Seeman, E. (2008). Bone quality: the material and structural basis of bone strength. *J Bone Miner Metab, 26*(1), 1-8. doi:10.1007/s00774-007-0793-5

Seeman, E., & Delmas, P. D. (2006). Bone quality--the material and structural basis of bone strength and fragility. *N Engl J Med, 354*(21), 2250-2261. doi:10.1056/NEJMra053077

Seguin, E. (1866). *Idiocy: and its treatment by the physiological method*. New York,: W. Wood & co.

Sinha, K. M., & Zhou, X. (2013). Genetic and molecular control of osterix in skeletal formation. *J Cell Biochem, 114*(5), 975-984. doi:10.1002/jcb.24439

Sturgeon, X., & Gardiner, K. J. (2011). Transcript catalogs of human chromosome 21 and orthologous chimpanzee and mouse regions. *Mamm Genome, 22*(5-6), 261-271. doi:10.1007/s00335-011-9321-y

Tang, J. Y. M., Luo, H., Wong, G. H. Y., Lau, M. M. Y., Joe, G. M., Tse, M. A., . . . Lum, T. Y. S. (2019). Bone mineral density from early to middle adulthood in persons with Down syndrome. *J Intellect Disabil Res*. doi:10.1111/jir.12608

Thompson, B. J., Bhansali, R., Diebold, L., Cook, D. E., Stolzenburg, L., Casagrande, A. S., . . . Crispino, J. D. (2015). DYRK1A controls the transition from proliferation to quiescence during lymphoid development by destabilizing Cyclin D3. *J Exp Med, 212*(6), 953-970. doi:10.1084/jem.20150002

Turner, C. H., & Burr, D. B. (1993). Basic biomechanical measurements of bone: a tutorial. *Bone, 14*(4), 595-608.

Turpin, R., & Lejeune, J. r. m. (1965). *Les chromosomes humains*. Paris,: Gauthier-Villars.

van Allen, M. I., Fung, J., & Jurenka, S. B. (1999). Health care concerns and guidelines for adults with Down syndrome. *Am J Med Genet, 89*(2), 100-110.

Wallace, J. M. (2014a). Skeletal Hard Tissue Biomechanics. In D. B. Burr, Allen, M. R. (Ed.), *Basic and Applied Bone Biology* (pp. 115-130): Elsevier Inc.

Wallace, J. M. (2014b). Skeletal Hard Tissue Biomechanics. In D. B. A. Burr, M. R. (Ed.), *Basic and Applied Bone Biology* (pp. 390): Elsevier Inc.

Wallace, J. M., Golcuk, K., Morris, M. D., & Kohn, D. H. (2009). Inbred strain-specific response to biglycan deficiency in the cortical bone of C57BL6/129 and C3H/He mice. *J Bone Miner Res, 24*(6), 1002-1012. doi:10.1359/jbmr.081259

Wallace, J. M., Rajachar, R. M., Chen, X. D., Shi, S., Allen, M. R., Bloomfield, S. A., . . . Kohn, D. H. (2006). The mechanical phenotype of biglycan-deficient mice is bone- and gender-specific. *Bone, 39*(1), 106-116. doi:10.1016/j.bone.2005.12.081

Wang, L., Mishina, Y., & Liu, F. (2015). Osterix-Cre transgene causes craniofacial bone development defect. *Calcif Tissue Int, 96*(2), 129-137. doi:10.1007/s00223-014-9945-5

Weijerman, M. E., & de Winter, J. P. (2010). Clinical practice. The care of children with Down syndrome. *Eur J Pediatr, 169*(12), 1445-1452. doi:10.1007/s00431-010-1253-0

Williams, A. D., Mjaatvedt, C. H., & Moore, C. S. (2008). Characterization of the cardiac phenotype in neonatal Ts65Dn mice. *Dev Dyn, 237*(2), 426-435. doi:10.1002/dvdy.21416

Wysokinski, D., Pawlowska, E., & Blasiak, J. (2015). RUNX2: A Master Bone Growth Regulator That May Be Involved in the DNA Damage Response. *DNA Cell Biol, 34*(5), 305-315. doi:10.1089/dna.2014.2688

Zhang, C. (2012). Molecular mechanisms of osteoblast-specific transcription factor Osterix effect on bone formation. *Beijing Da Xue Xue Bao Yi Xue Ban, 44*(5), 659-665.

Zhou, X., Zhang, Z., Feng, J. Q., Dusevich, V. M., Sinha, K., Zhang, H., . . . de Crombrugghe, B. (2010). Multiple functions of Osterix are required for bone growth and homeostasis in postnatal mice. *Proc Natl Acad Sci U S A, 107*(29), 12919-12924. doi:10.1073/pnas.0912855107